

Latest results from MiniBooNE

E. D. Zimmerman
University of Colorado

SLAC Summer Institute Topical Conference
August 10, 2010

My last SSI talk

- SSI 2000
- MiniBooNE construction had just begun

E. Zimmerman, SSI 2000

RECENT RESULTS
FROM E815 (NuTeV)

E. D. ZIMMERMAN

COLUMBIA UNIVERSITY
NEW YORK, NEW YORK

SLAC SUMMER INSTITUTE
AUGUST 24, 2000

Latest Results from MiniBooNE

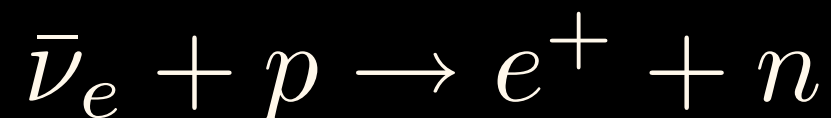
- MiniBooNE
- Neutrino cross-sections
 - Quasielastic and elastic scattering
 - Hadron production channels
- Neutrino Oscillations
- Antineutrino Oscillations

Motivating MiniBooNE: LSND

Liquid Scintillator Neutrino Detector

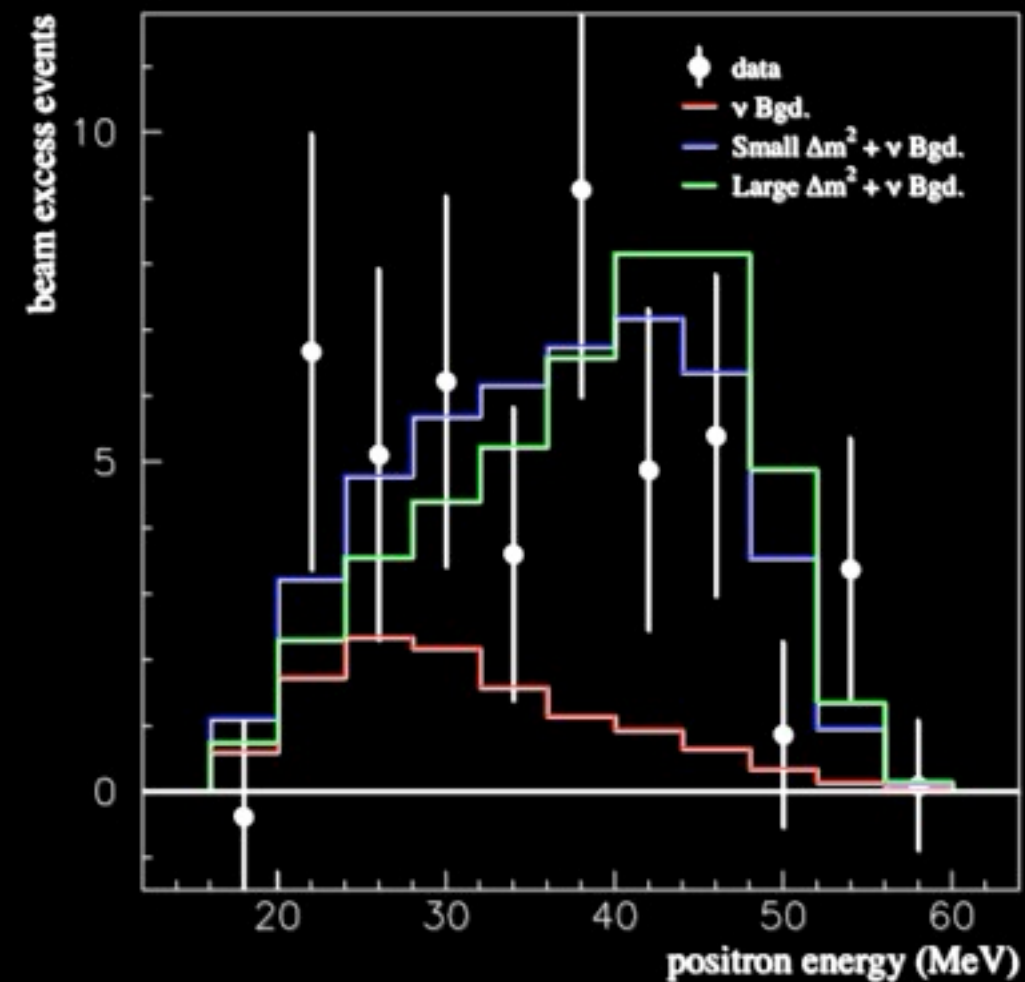
- Stopped π^+ beam at Los Alamos LAMPF produces $\nu_e, \nu_\mu, \bar{\nu}_\mu$ but no $\bar{\nu}_e$ (due to π^- capture).

Search for $\bar{\nu}_e$ appearance via reaction:



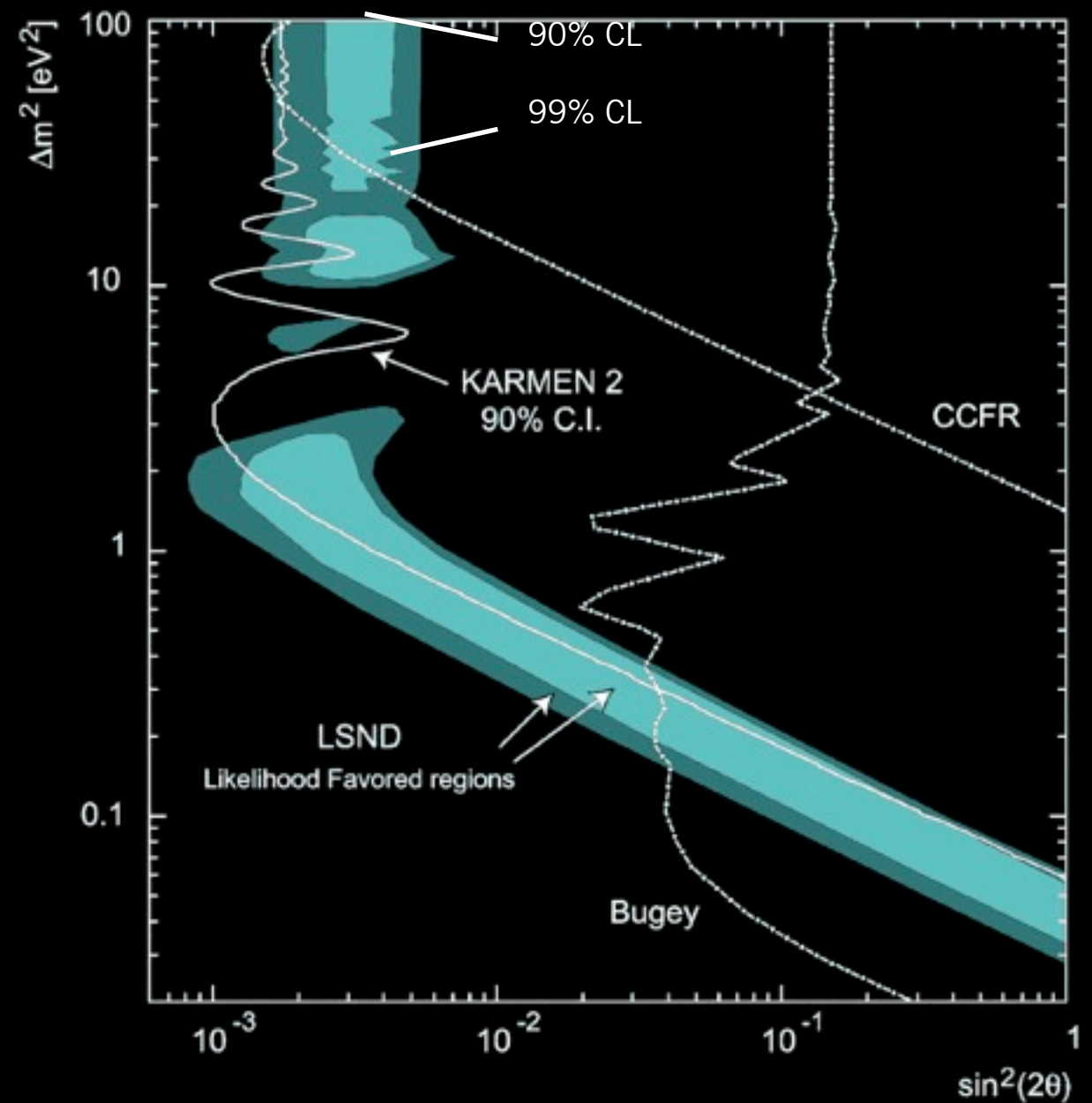
- Neutron thermalizes, captures $\rightarrow 2.2$ MeV γ -ray
- Look for the delayed coincidence.
- Major background non-beam (measured, subtracted)
- 3.8 standard dev. excess above background.
- Oscillation probability:

$$P(\bar{\nu}_\mu \rightarrow \bar{\nu}_e) = (2.5 \pm 0.6_{\text{stat}} \pm 0.4_{\text{syst}}) \times 10^{-3}$$



LSND oscillation signal

- LSND “allowed region” shown as band
- KARMEN2 is a similar experiment with a slightly smaller L/E; they see no evidence for oscillations. Excluded region is to right of curve.



The Overall Picture

LSND	$\Delta m^2 > 0.1 \text{eV}^2$	$\bar{\nu}_\mu \leftrightarrow \bar{\nu}_e$
Atmos.	$\Delta m^2 \approx 2 \times 10^{-3} \text{eV}^2$	$\nu_\mu \leftrightarrow \nu_\tau$
Solar	$\Delta m^2 \approx 10^{-4} \text{eV}^2$	$\nu_e \leftrightarrow \nu_\tau$

With only 3 masses, can't construct 3 Δm^2 values of different orders of magnitude!

- Is there a fourth neutrino?
 - If so, it can't interact weakly at all because of Z^0 boson resonance width measurements consistent with only three neutrinos.
- We need one of the following:
 - A "sterile" neutrino sector
 - Discovery that one of the observed effects is not oscillations
 - A new idea

MiniBooNE: E898 at Fermilab

- Purpose is to test LSND with:
 - Higher energy
 - Different beam
 - Different oscillation signature
 - Different systematics
- $L=500$ meters, $E=0.5-1$ GeV: same L/E as LSND.

Oscillation Signature at MiniBooNE

- Oscillation signature is charged-current quasielastic scattering:



- Dominant backgrounds to oscillation:

- Intrinsic ν_e in the beam

$\pi \rightarrow \mu \rightarrow \nu_e$ in beam

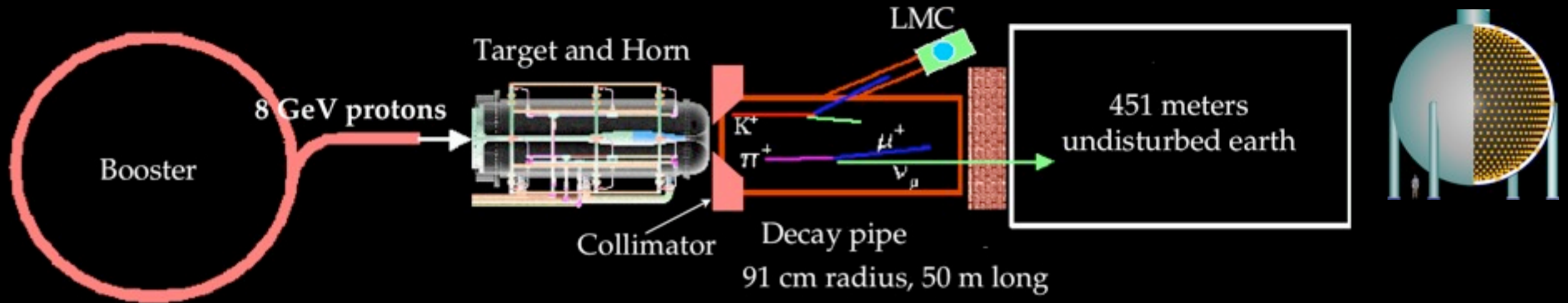
$K^+ \rightarrow \pi^0 e^+ \nu_e, K_L^0 \rightarrow \pi^0 e^\pm \nu_e$ in beam

- Particle misidentification in detector

Neutral current resonance:

$\Delta \rightarrow \pi^0 \rightarrow \gamma\gamma$ or $\Delta \rightarrow n\gamma$, mis-ID as e

MiniBooNE Beamline



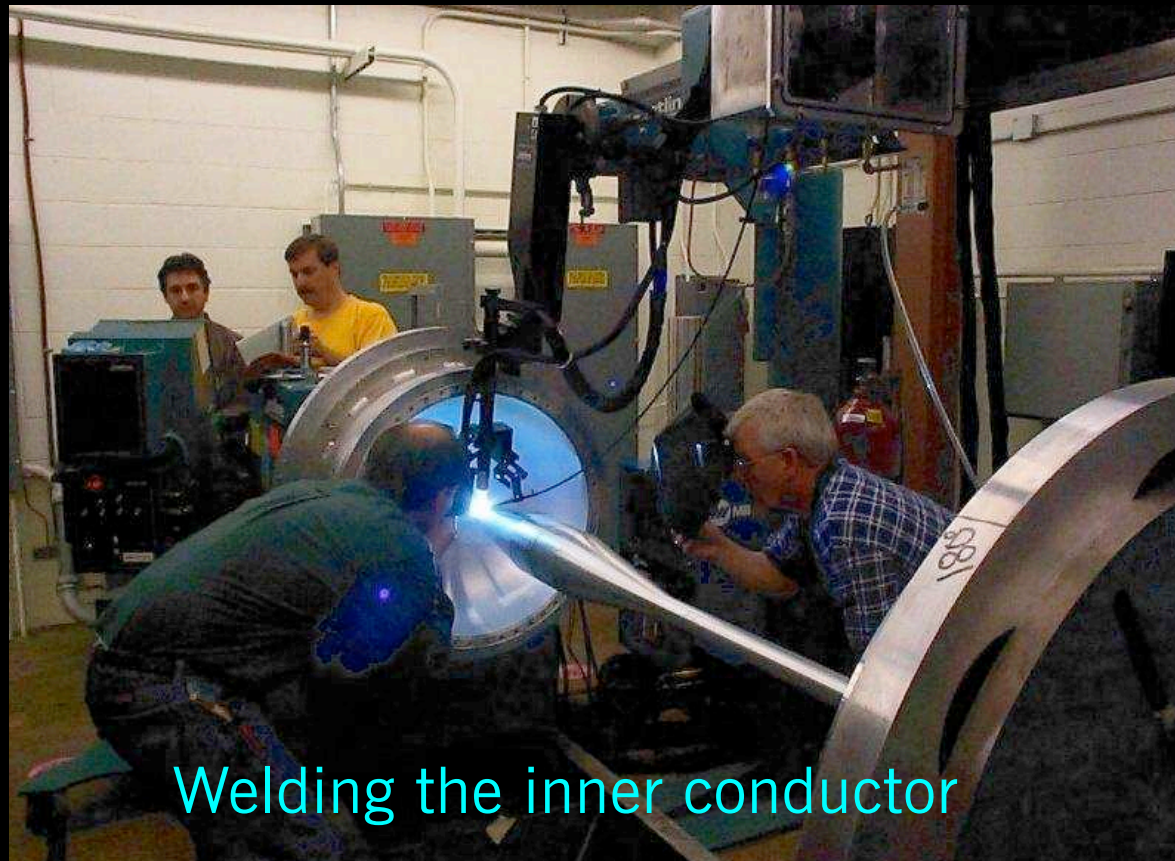
- 8 GeV primary protons come from Booster accelerator at Fermilab
- Booster provides about 5 pulses per second, 5×10^{12} protons per $1.6 \mu\text{s}$ pulse under optimum conditions

Secondary beam: horn and target

- Target is beryllium, 71 cm (1.7λ).
- Cooling tube and target are cantilevered into the neck of the horn.
- MiniBooNE horn runs at 174 kA, 140 μ s pulse. Can focus π^+ for neutrinos or π^- for antineutrinos.



Target assembly

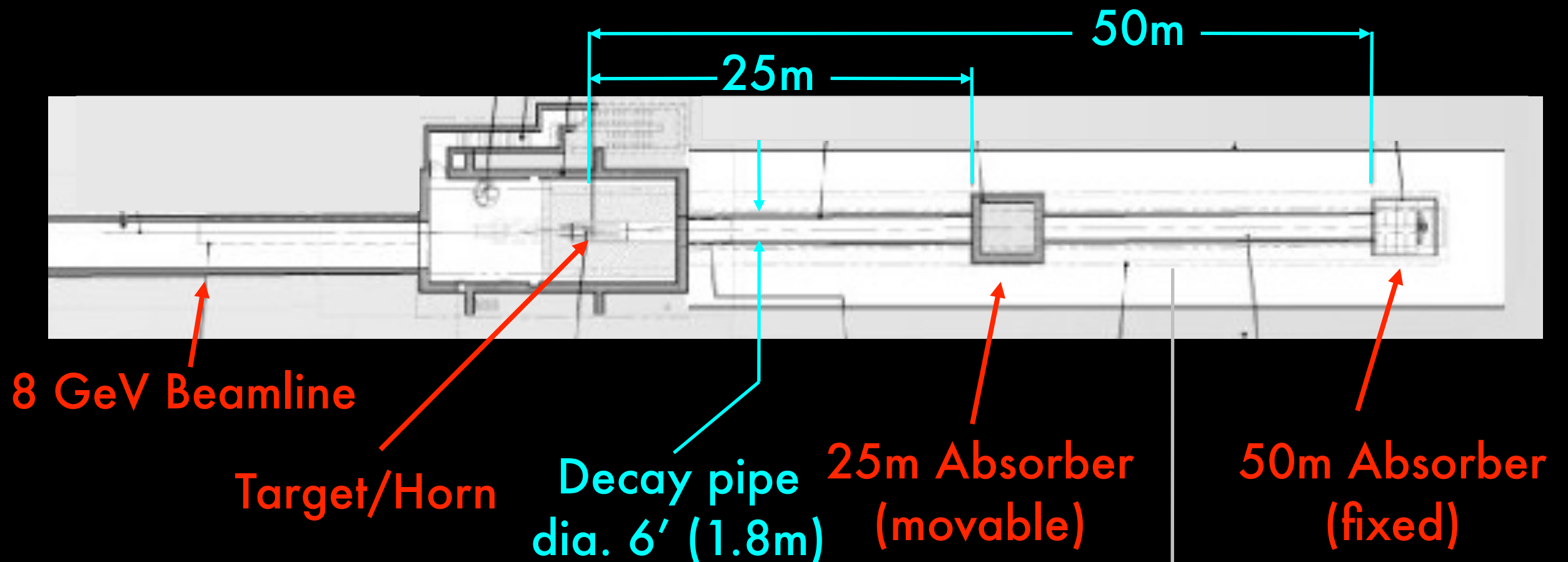


Welding the inner conductor



Assembled horn

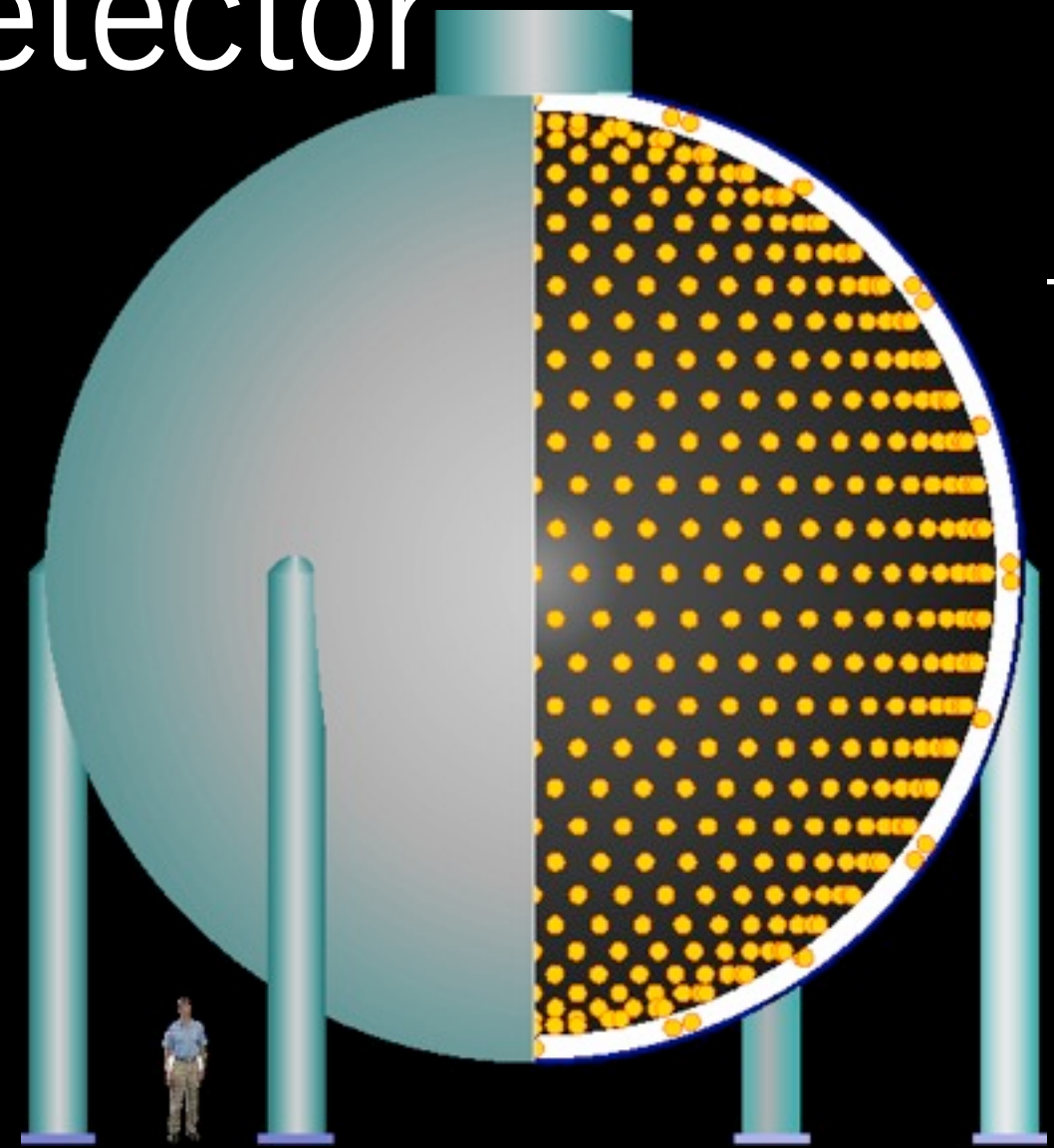
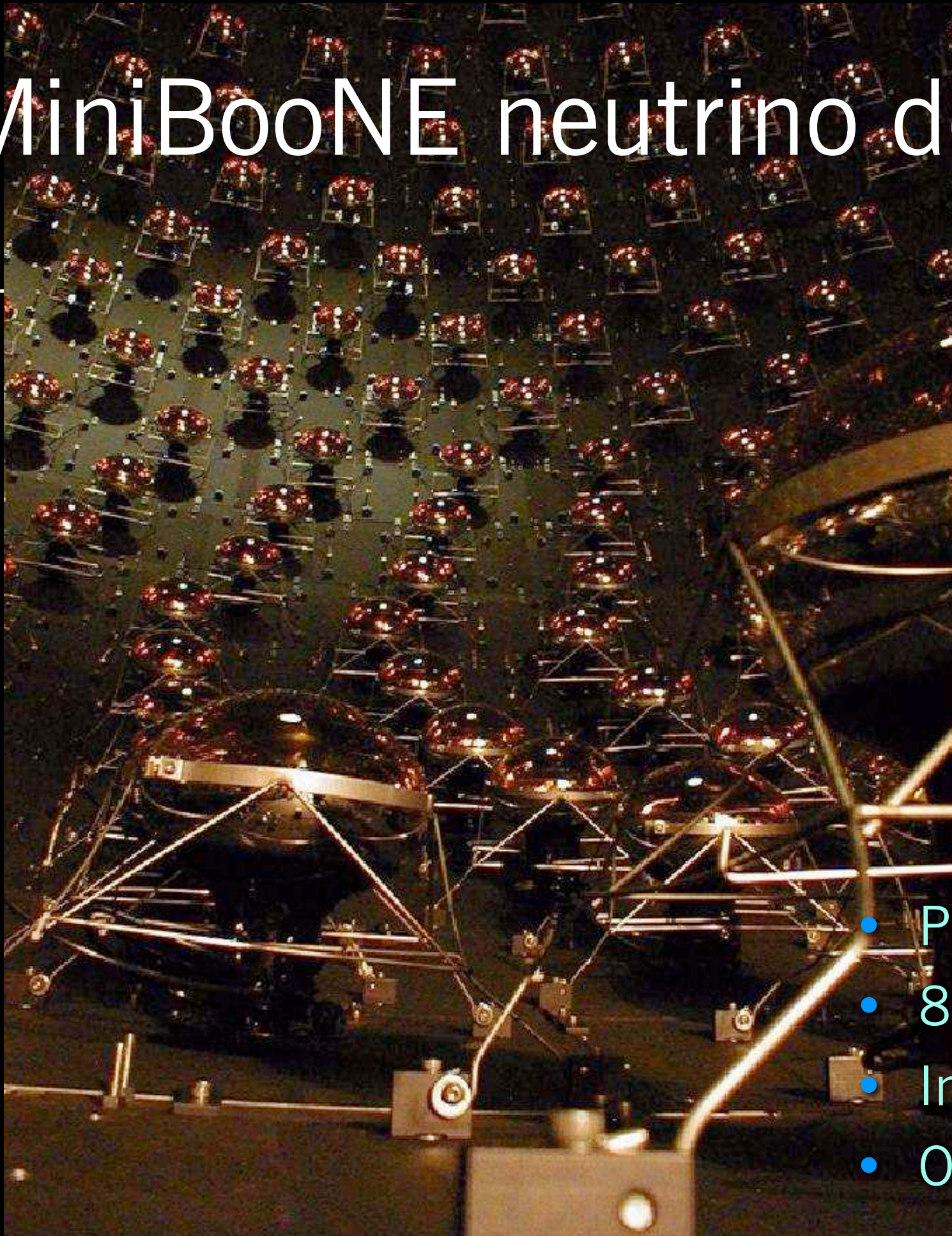
Decay Pipe and absorber



- Decay region is filled with stagnant air shared with target pile.

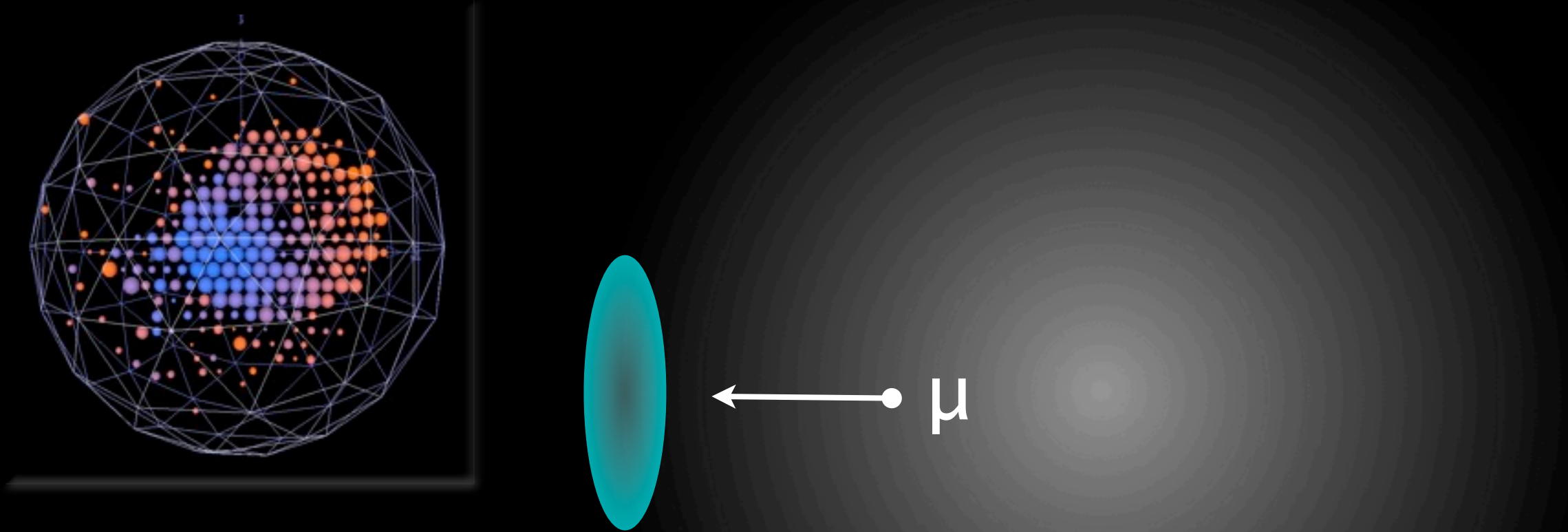
- Shielding provided by gravel fill and earth berm above decay pipe

MiniBooNE neutrino detector



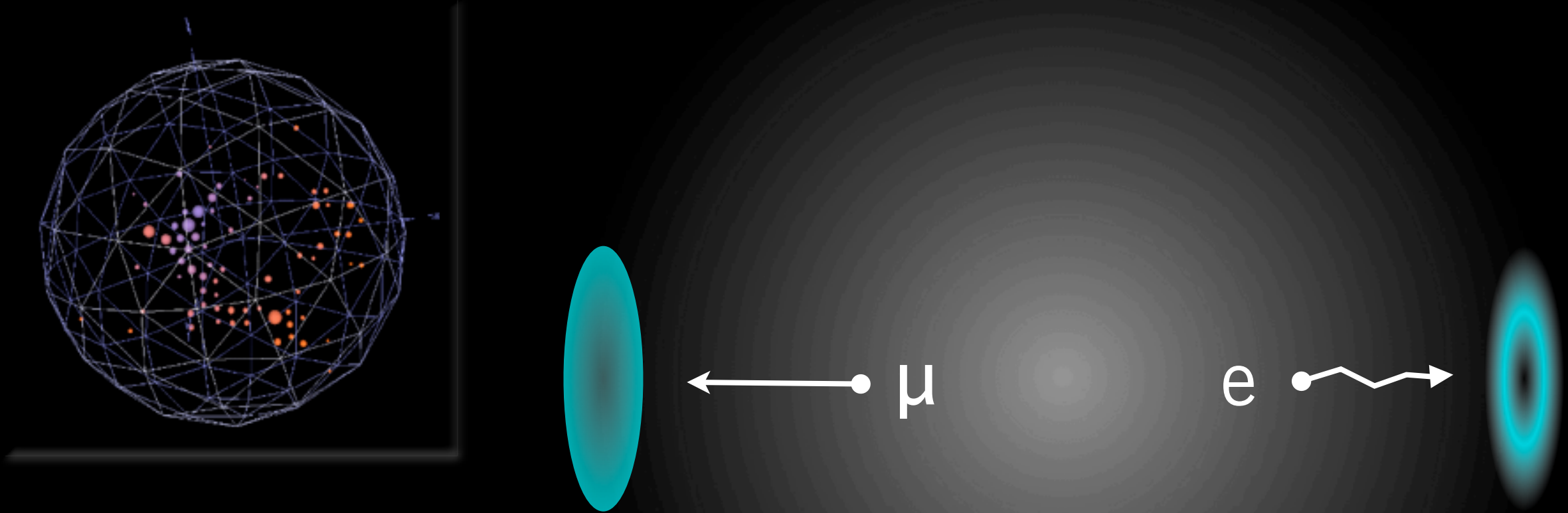
- Pure mineral oil
- 800 tons; 40 ft diameter
- Inner volume: 1280 8" PMTs
- Outer veto volume: 240 PMTs

Cherenkov ring characteristics: muons



- Muons have sharp filled in Cherenkov rings.

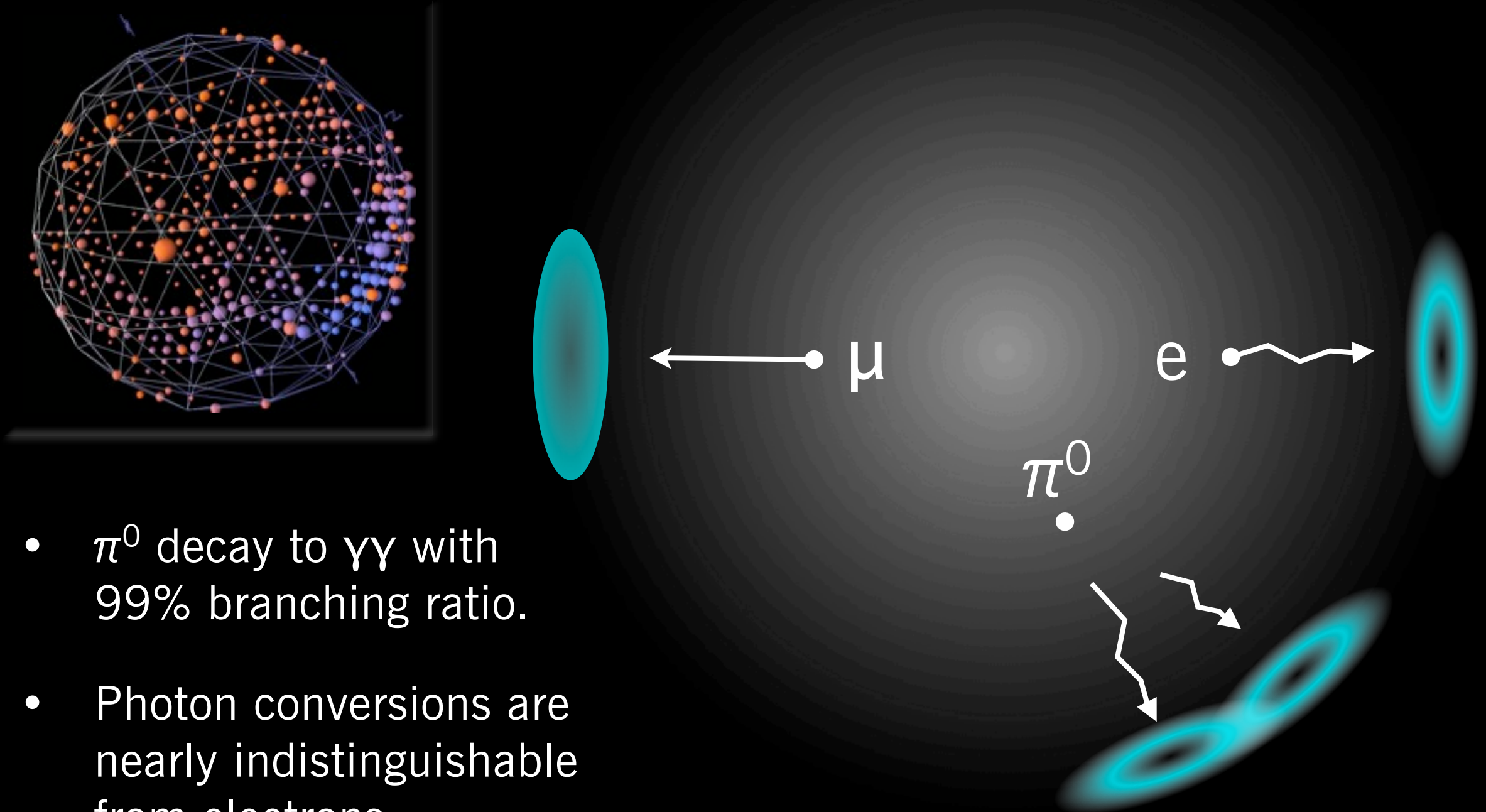
Cherenkov ring characteristics: electrons



- Electrons undergo more scattering and produce “fuzzy” rings.

Cherenkov ring characteristics:

π^0



- π^0 decay to $\gamma\gamma$ with 99% branching ratio.
- Photon conversions are nearly indistinguishable from electrons.

MiniBooNE's track-based reconstruction

- A detailed analytic model of extended-track light production and propagation in the tank predicts the probability distribution for charge and time on each PMT for individual muon or electron/photon tracks.
- Prediction based on seven track parameters: vertex (x,y,z) , time, energy, and direction $(\theta, \varphi) \Leftrightarrow (U_x, U_y, U_z)$.
- Fitting routine varies parameters to determine 7-vector that best predicts the actual hits in a data event
- Particle identification comes from ratios of likelihoods from fits to different parent particle hypotheses

Beam/Detector Operation

- Fall 2002 - Jan 2006: Neutrino mode (first oscillation analysis).
- Jan 2006 - 2011(?): Antineutrino mode
 - (Interrupted by short Fall 2007 - April 2008 neutrino running)
- Present analyses use:
 - $\geq 5.7E20$ protons on target for neutrino analyses
 - $5.66E20$ protons on target for antineutrino analyses
 - Over one million neutrino interactions recorded: by far the largest data set in this energy range

Neutrino scattering cross-sections

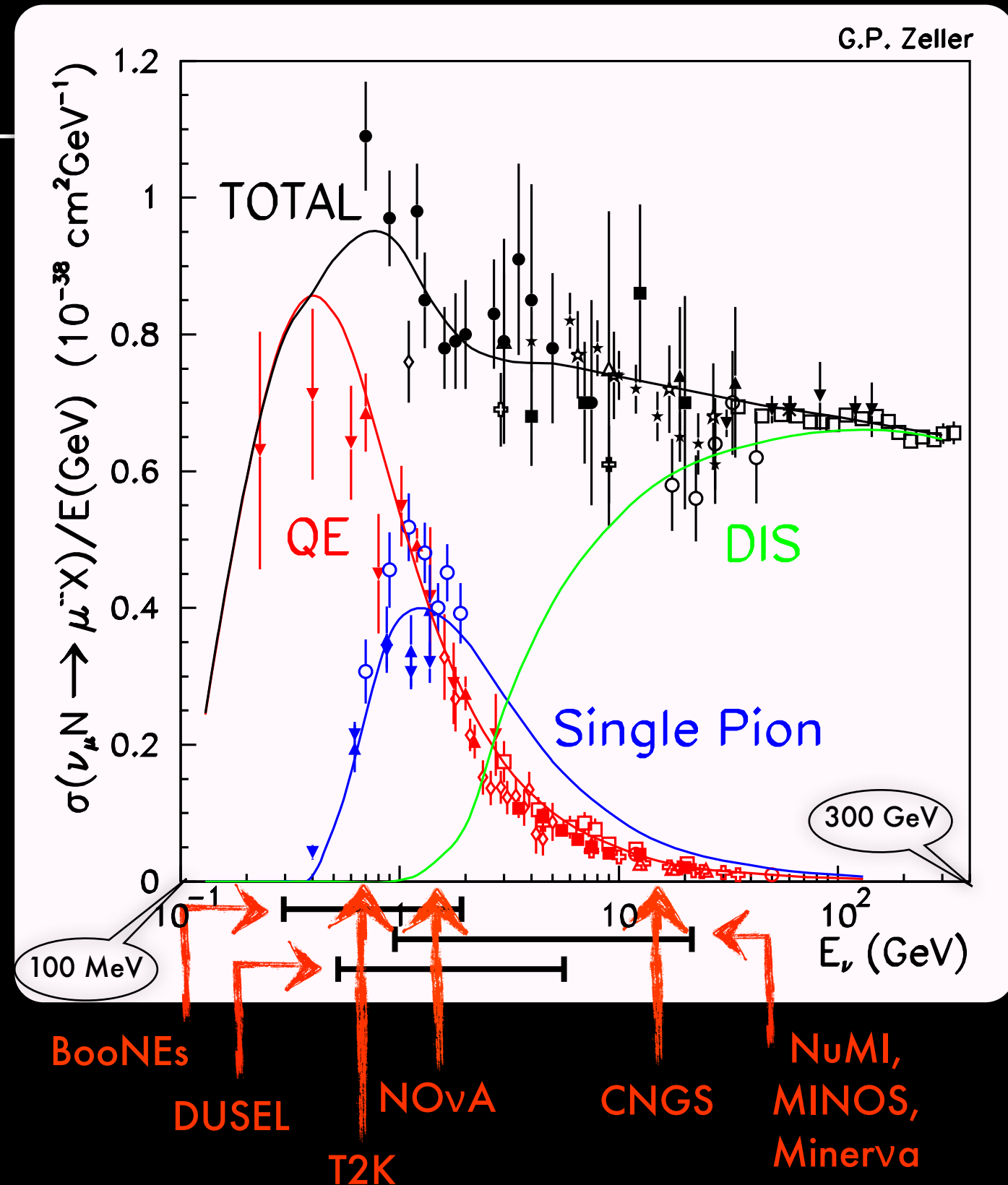
- To understand the flavor physics of neutrinos (*i.e.* oscillations), it is critical to understand the physics of neutrino interactions
- This is a real challenge for most neutrino experiments:
 - Broadband beams
 - Large backgrounds to most interaction channels
 - Nuclear effects (which complicate even the definition of the scattering processes!)

Scattering cross-sections

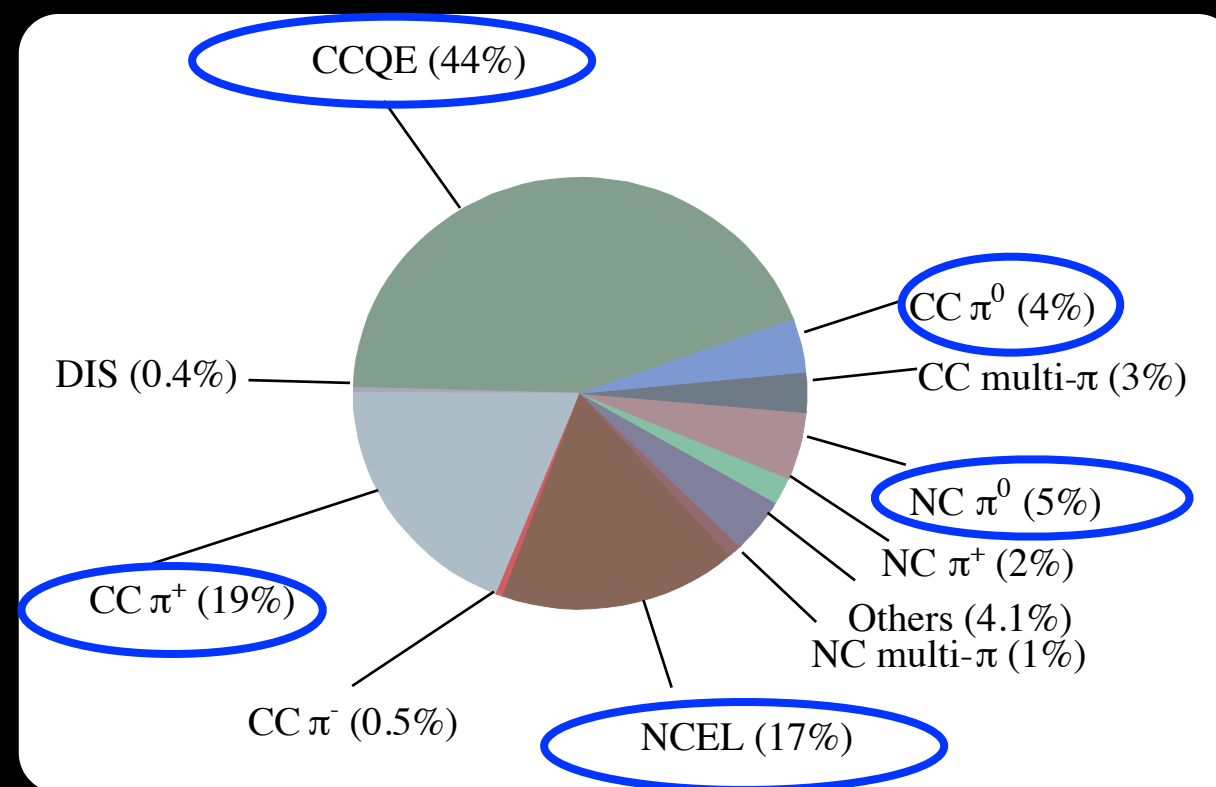
for ν_μ

The state of knowledge of ν_μ interactions before the current generation of experiments:

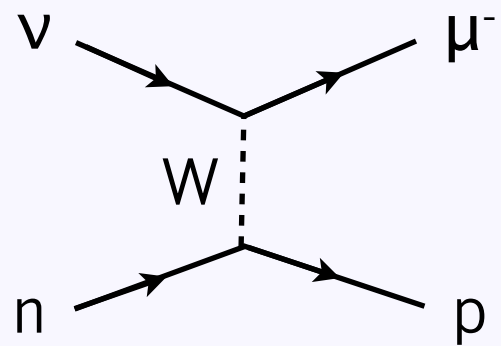
- Lowest energy ($E < 500$ MeV) is dominated by CCQE.
- Moderate energies (500 MeV $< E < 5$ GeV) have lots of single pion production.
- High energies ($E > 5$ GeV) are completely dominated by deep inelastic scattering (DIS).
- Most data over 20 years old, and on light targets (deuterium).
- Current and future experiments use nuclear targets from C to Pb; almost no data available.



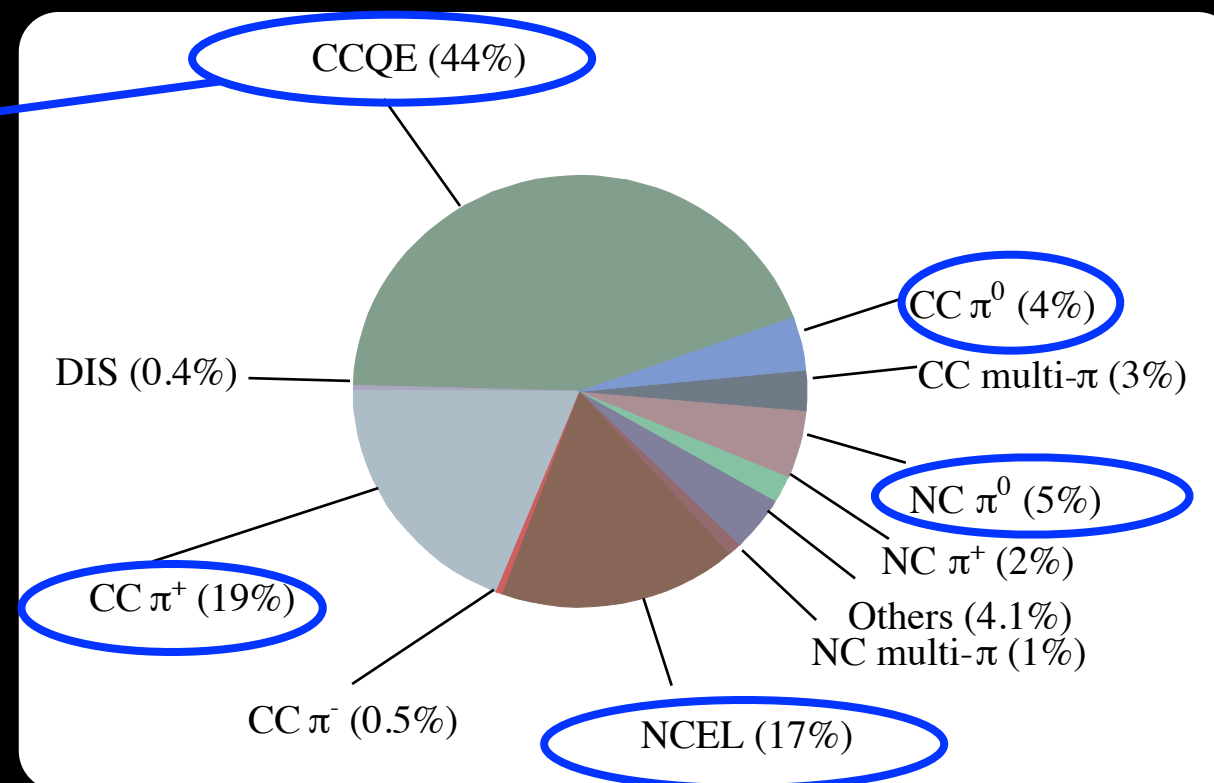
Dominant interaction channels at MiniBooNE



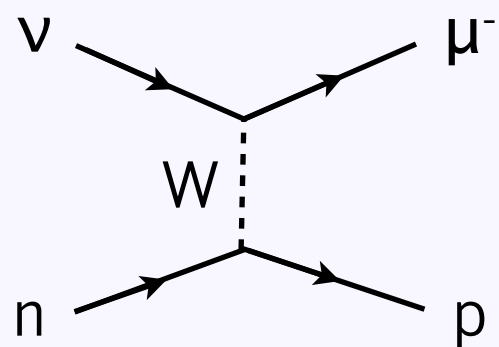
Dominant interaction channels at MiniBooNE



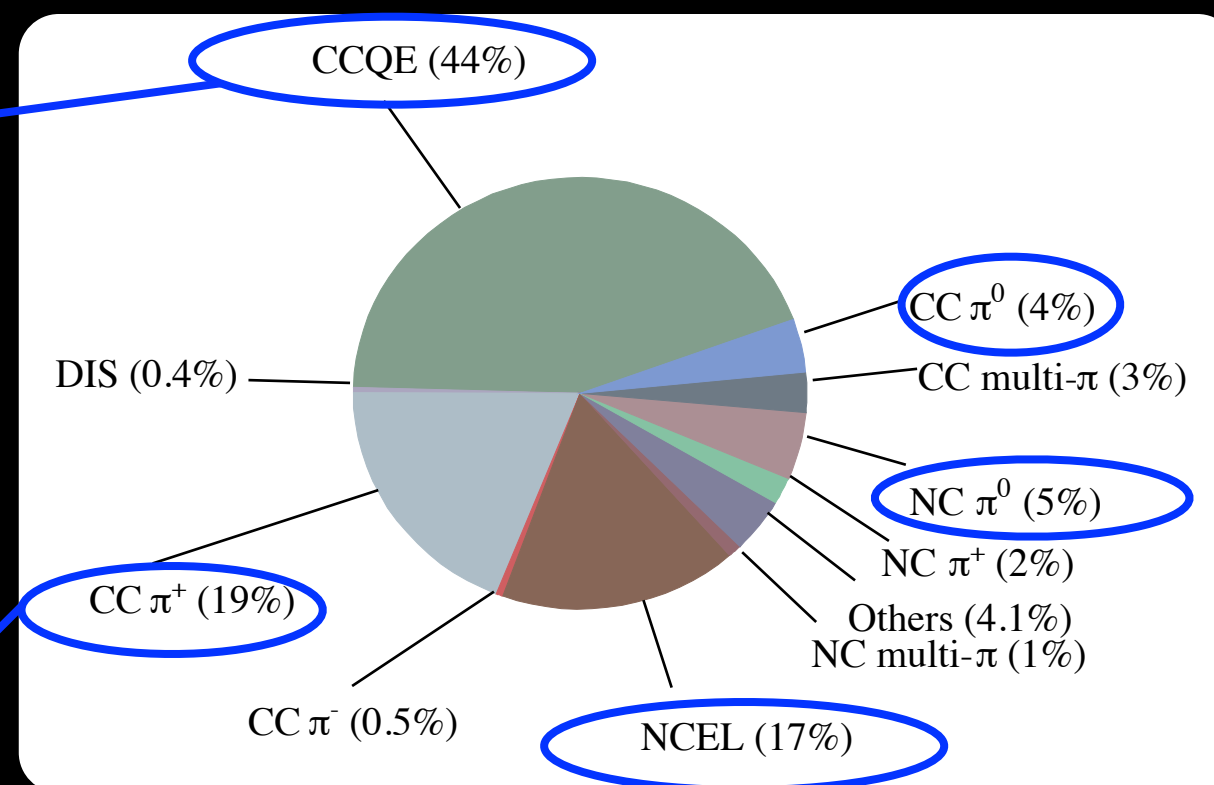
Charged-current quasielastic



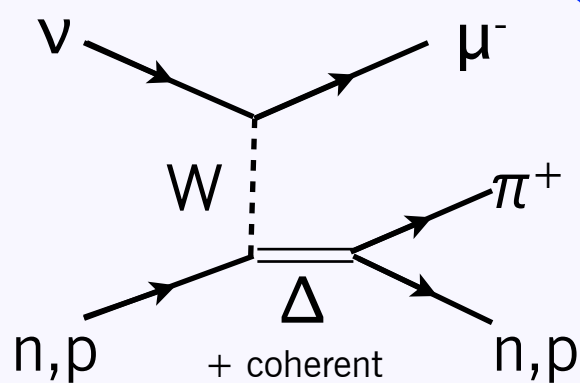
Dominant interaction channels at MiniBooNE



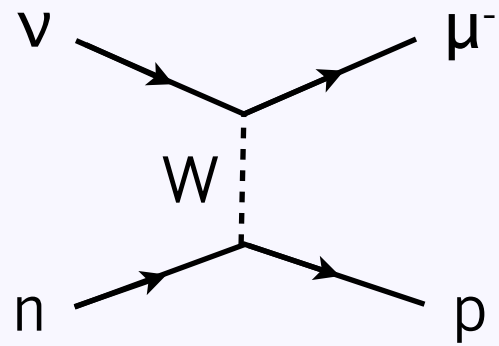
Charged-current quasielastic



Charged-current π^+ production

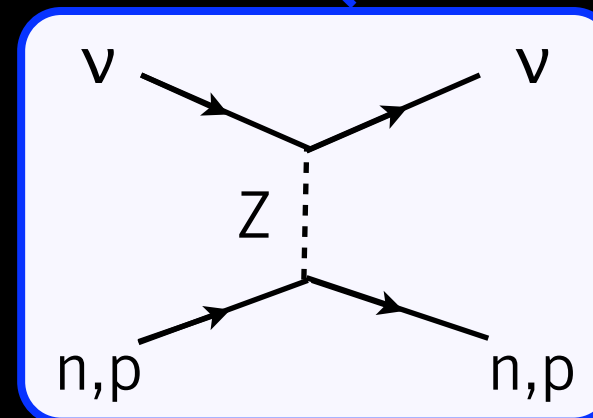
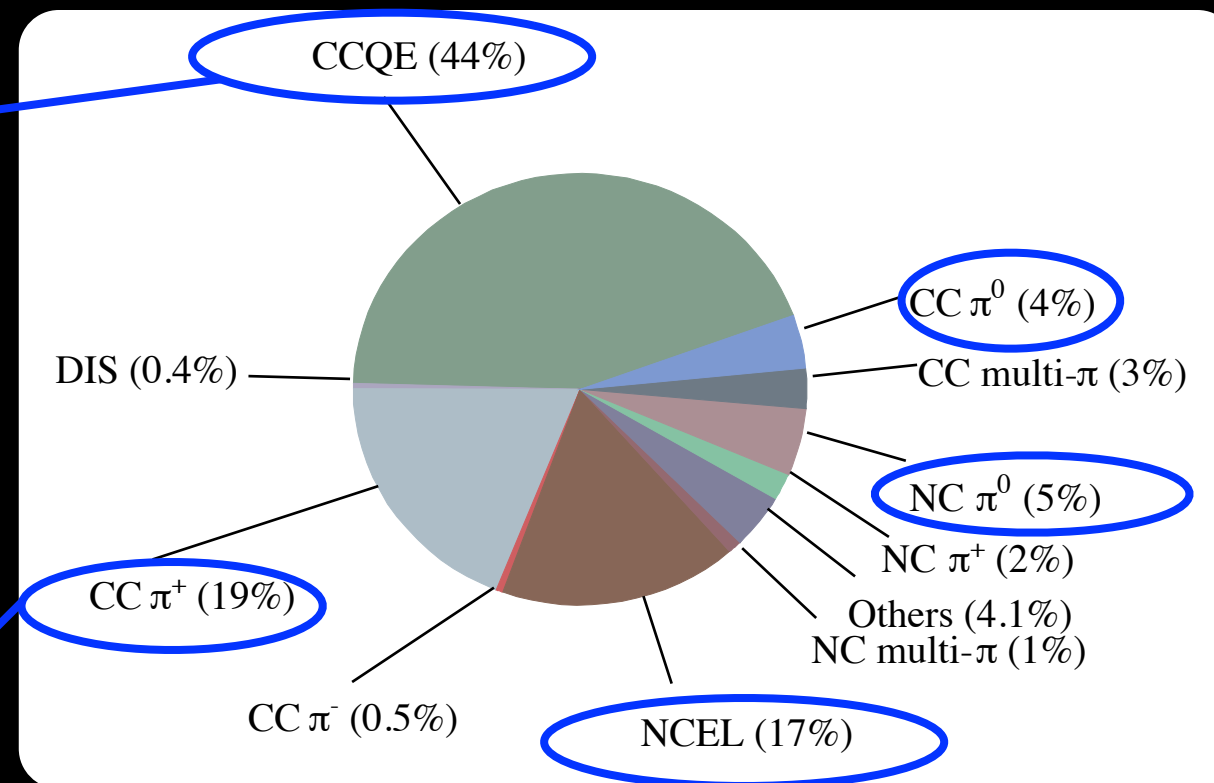
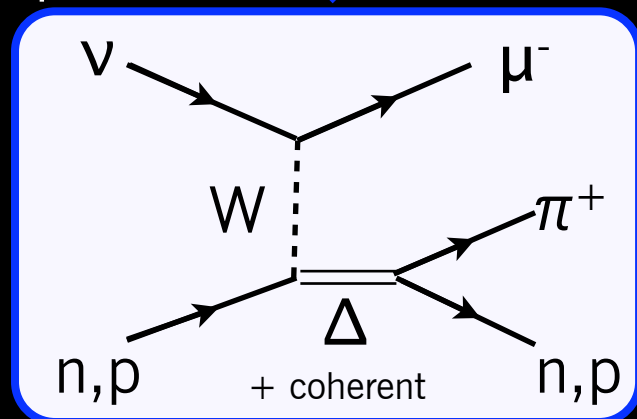


Dominant interaction channels at MiniBooNE



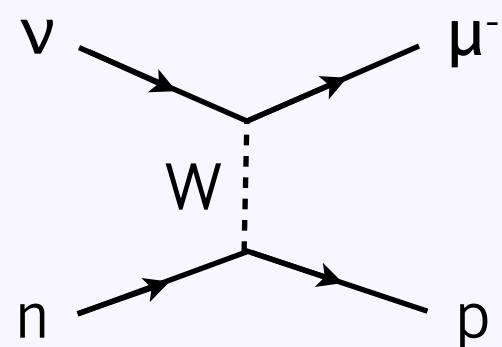
Charged-current quasielastic

Charged-current π^+ production

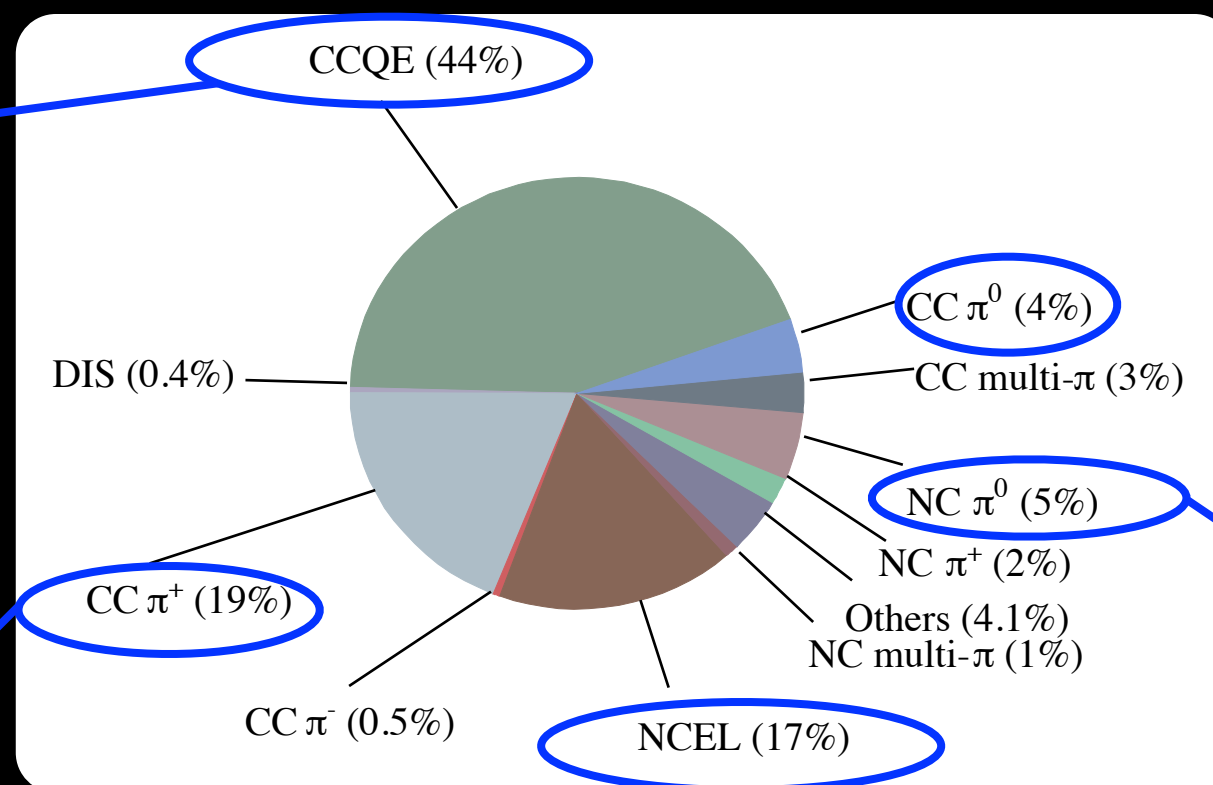


Neutral-current elastic

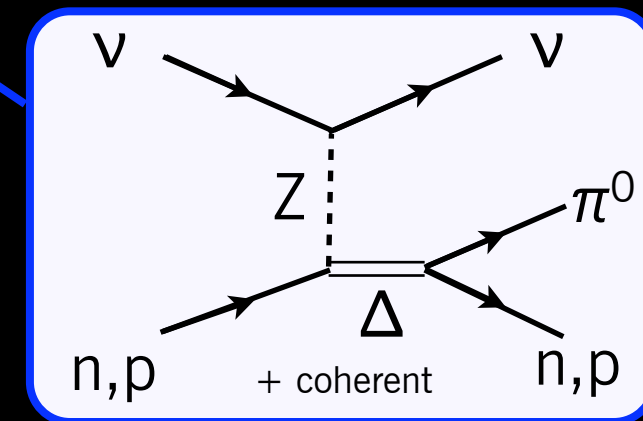
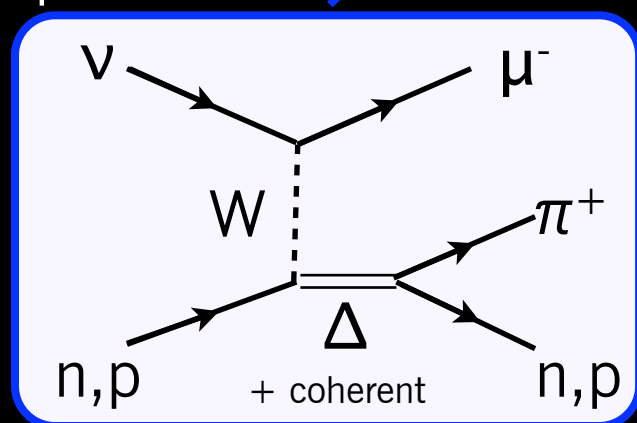
Dominant interaction channels at MiniBooNE



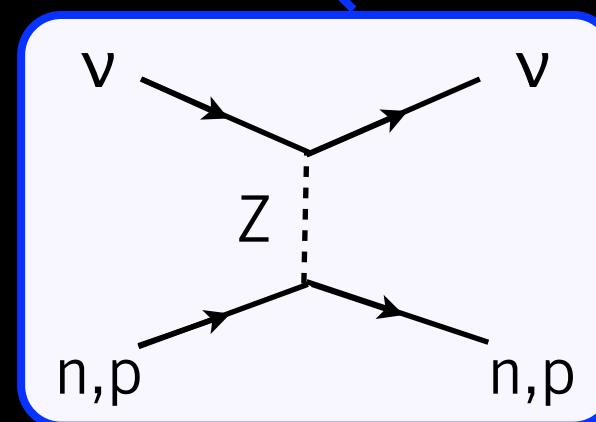
Charged-current quasielastic



Charged-current π^+ production

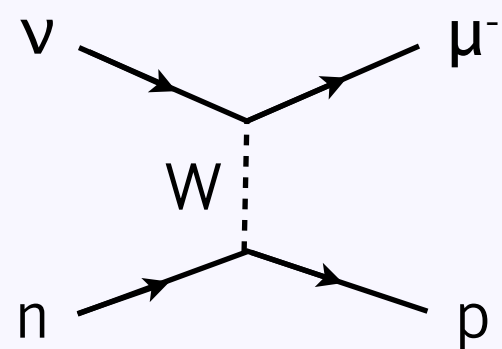


Neutral-current π^0 production



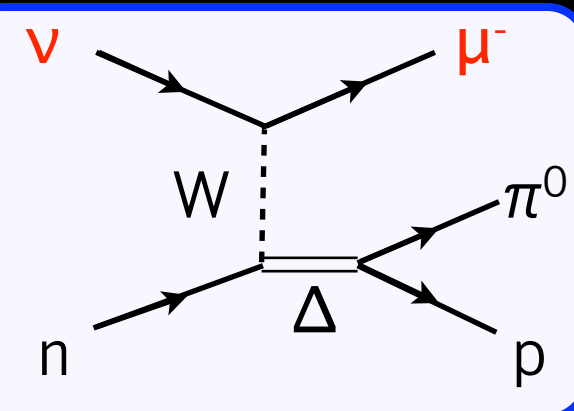
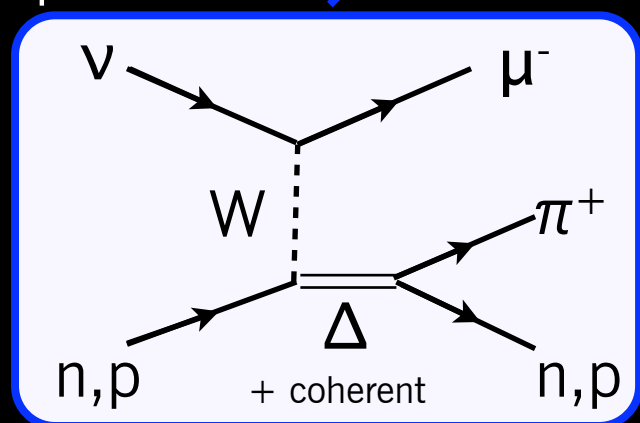
Neutral-current elastic

Dominant interaction channels at MiniBooNE

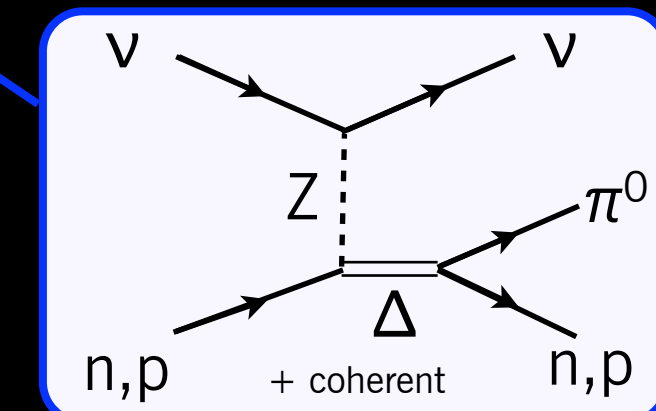


Charged-current quasielastic

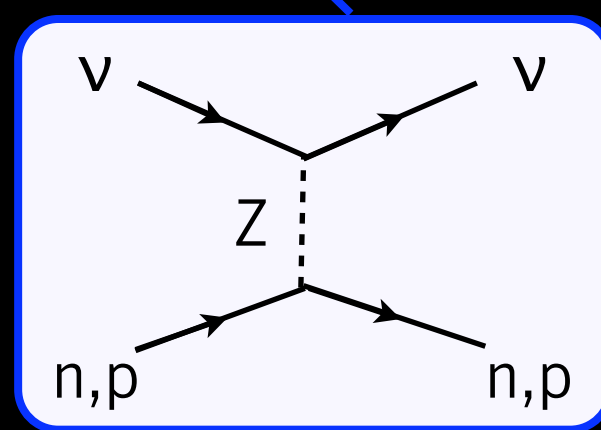
Charged-current π^+ production



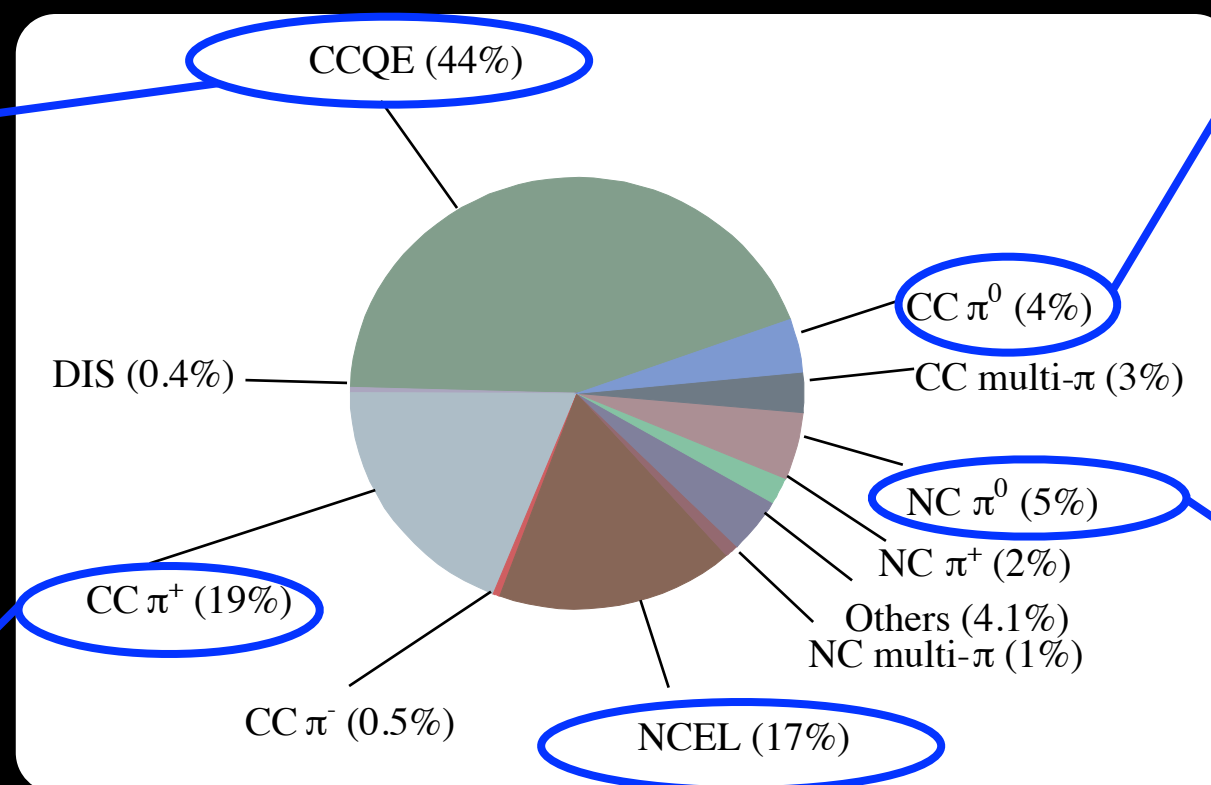
Charged-current π^0 production



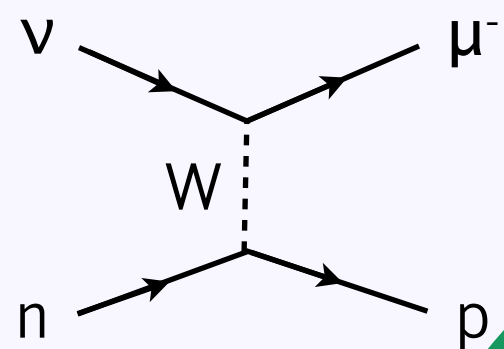
Neutral-current π^0 production



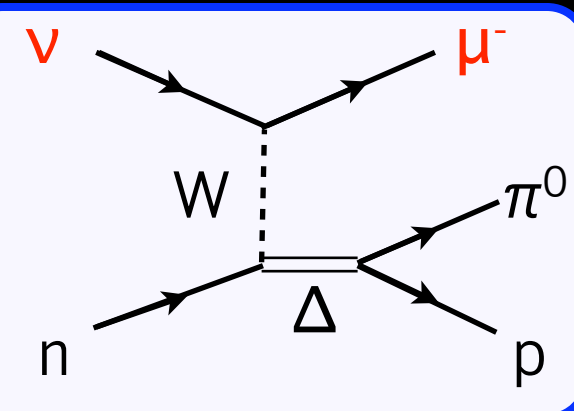
Neutral-current elastic



Dominant interaction channels at MiniBooNE

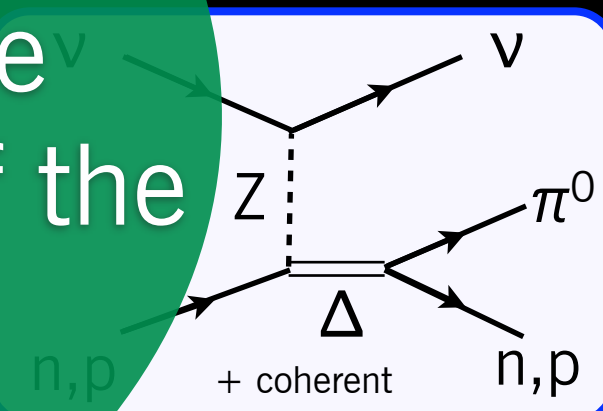
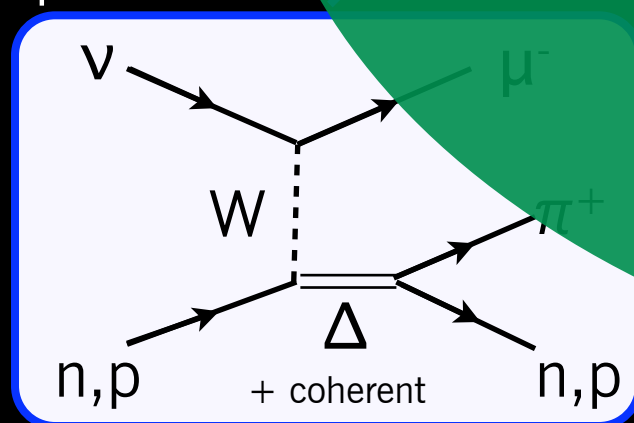


Charged-current quasielastic

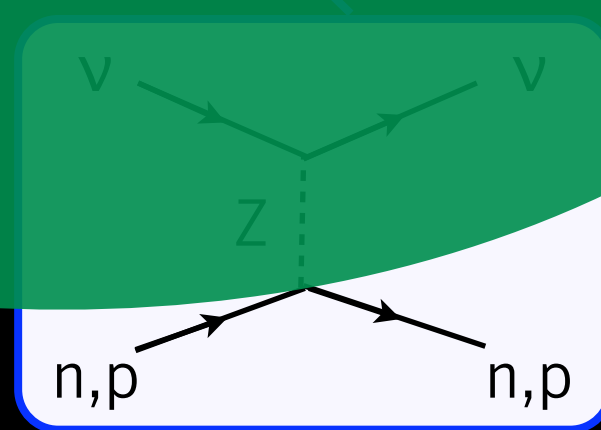


Charged-current π^0 production

Charged-current π^+ production



Neutral-current π^0 production



Neutral-current elastic

MiniBooNE has measured cross-sections for all of these exclusive channels, which add up to 89% of the total event rate

CCQE (44%)

CC π^0 (4%)

CC multi- π (3%)

NC π^0 (5%)

Others (4.1%)

NC multi- π (2%)

NCBEL (17%)

DIS (0.4%)

CC π^+ (19%)

CC π^0 (19%)

Critical for measuring cross-sections: well-understood flux

- Detailed MC simulations of target+horn+decay region, using π production tables from dedicated measurements: PRD **79** 072002 (2009).
- **No flux tuning based on MB data**
- Most important π production measurements from HARP(at CERN) at 8.9 GeV/c beam momentum (as MB), 5% int. length Be target (Eur.Phys.J.C52 (2007)29)
- Error on HARP data (7%) is dominant contribution to flux uncertainty
- Overall 9% flux uncertainty, dominates cross section normalization (“scale”) error

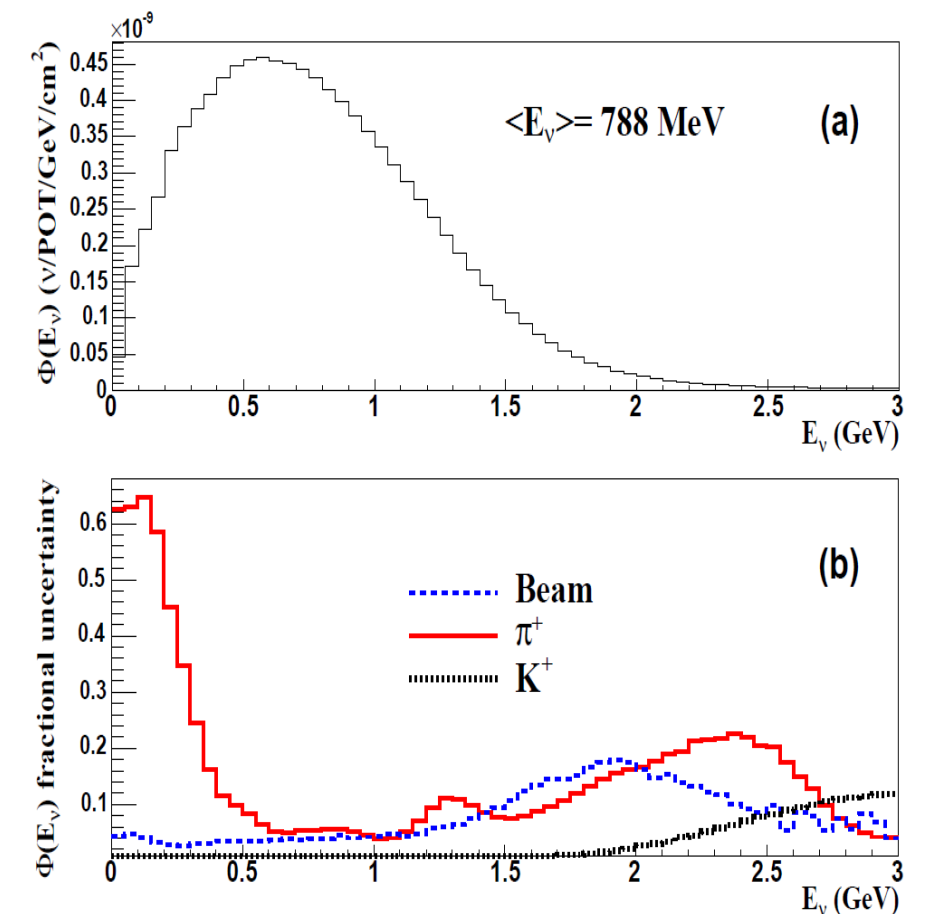


FIG. 2: (color online) Predicted ν_μ flux at the MiniBooNE detector (a) along with the fractional uncertainties grouped into various contributions (b). The integrated flux is $5.16 \times 10^{-10} \nu_\mu/\text{POT}/\text{cm}^2$ ($0 < E_\nu < 3$ GeV) with a mean energy of 788 MeV. Numerical values corresponding to the top plot are provided in Table V in the Appendix.

MiniBooNE cross-section measurements

- NC π^0
- CC π^0
- CC π^+
- CC Quasielastic
- NC Elastic
- CC Inclusive

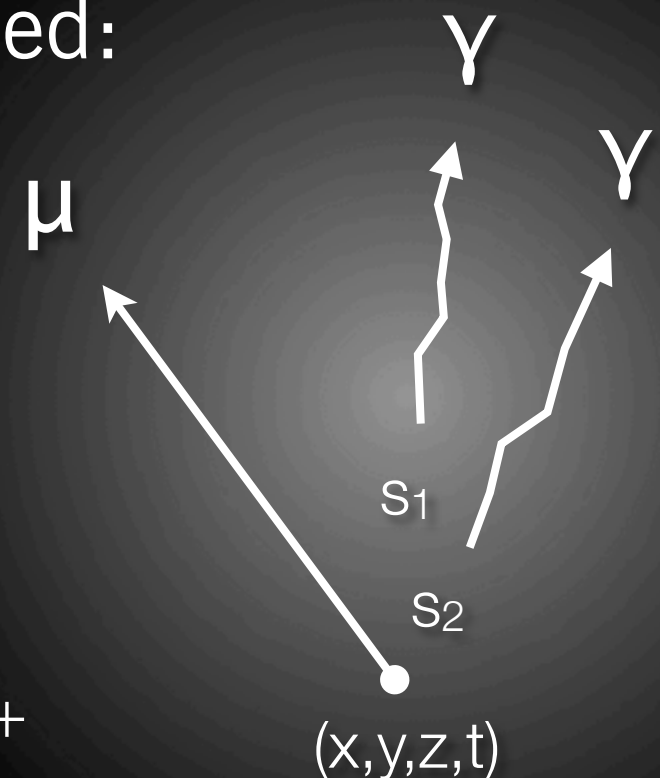
MiniBooNE cross-section measurements

- ~~NC π^0~~
- CC π^0
- CC π^+
- CC Quasielastic
- ~~NC Elastic~~
- ~~CC Inclusive~~

Due to limited time, only discussing charged-current exclusive modes here.

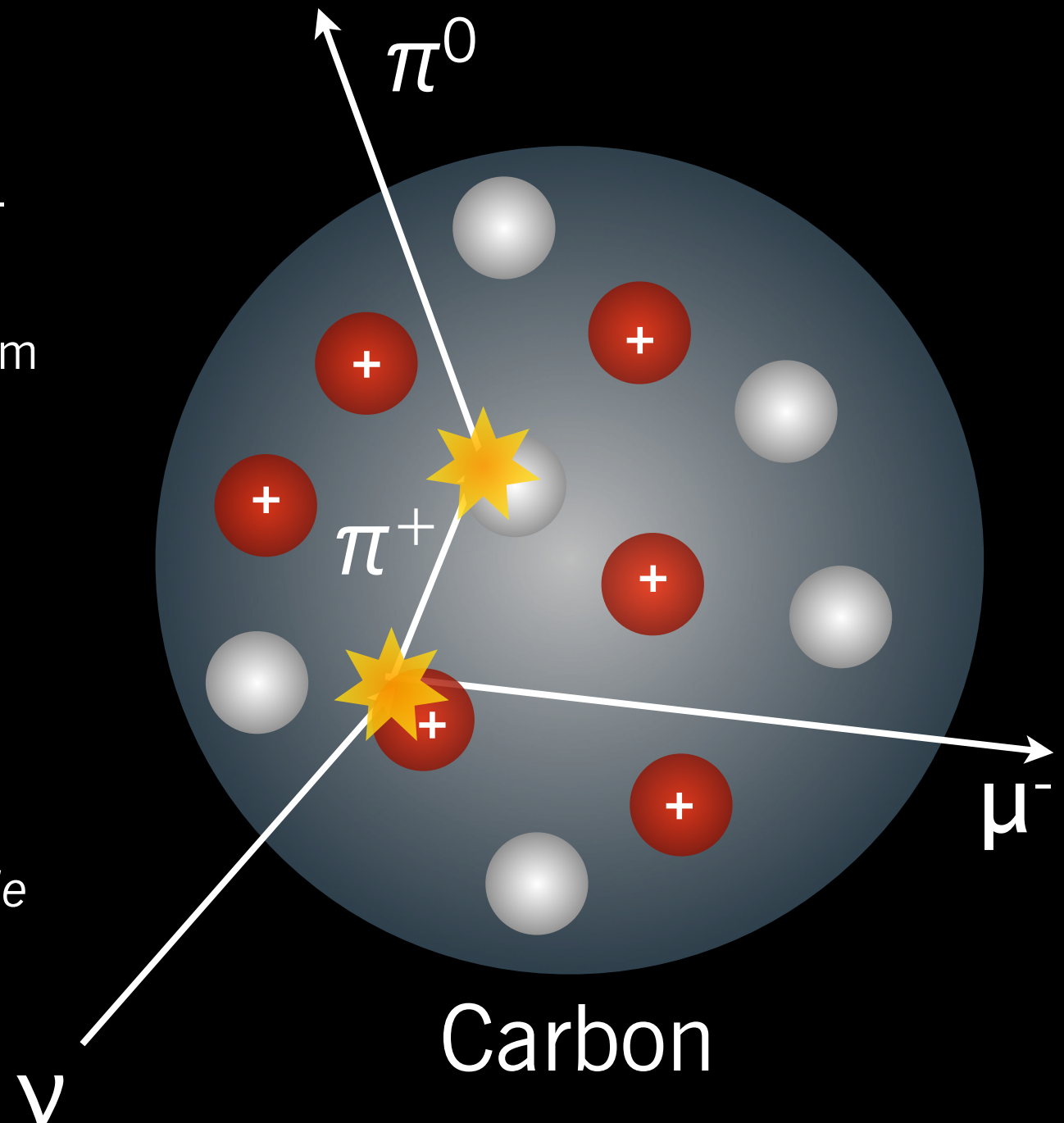
Charged-current π^0 production

- Least common interaction for which we do exclusive measurement
- Uniquely, proceeds only via resonance:
 $\nu + n \rightarrow \mu + \Delta \rightarrow \mu + p + \pi^0$
- Challenging 15-parameter, 3-ring fit needed:
 - Event vertex: (x, y, z, t)
 - Muon: (E, θ, φ)
 - 1st photon: (E, θ, φ, s)
 - 2nd photon: (E, θ, φ, s)
- Relatively high backgrounds (mostly $CC\pi^+$ which we measure separately)



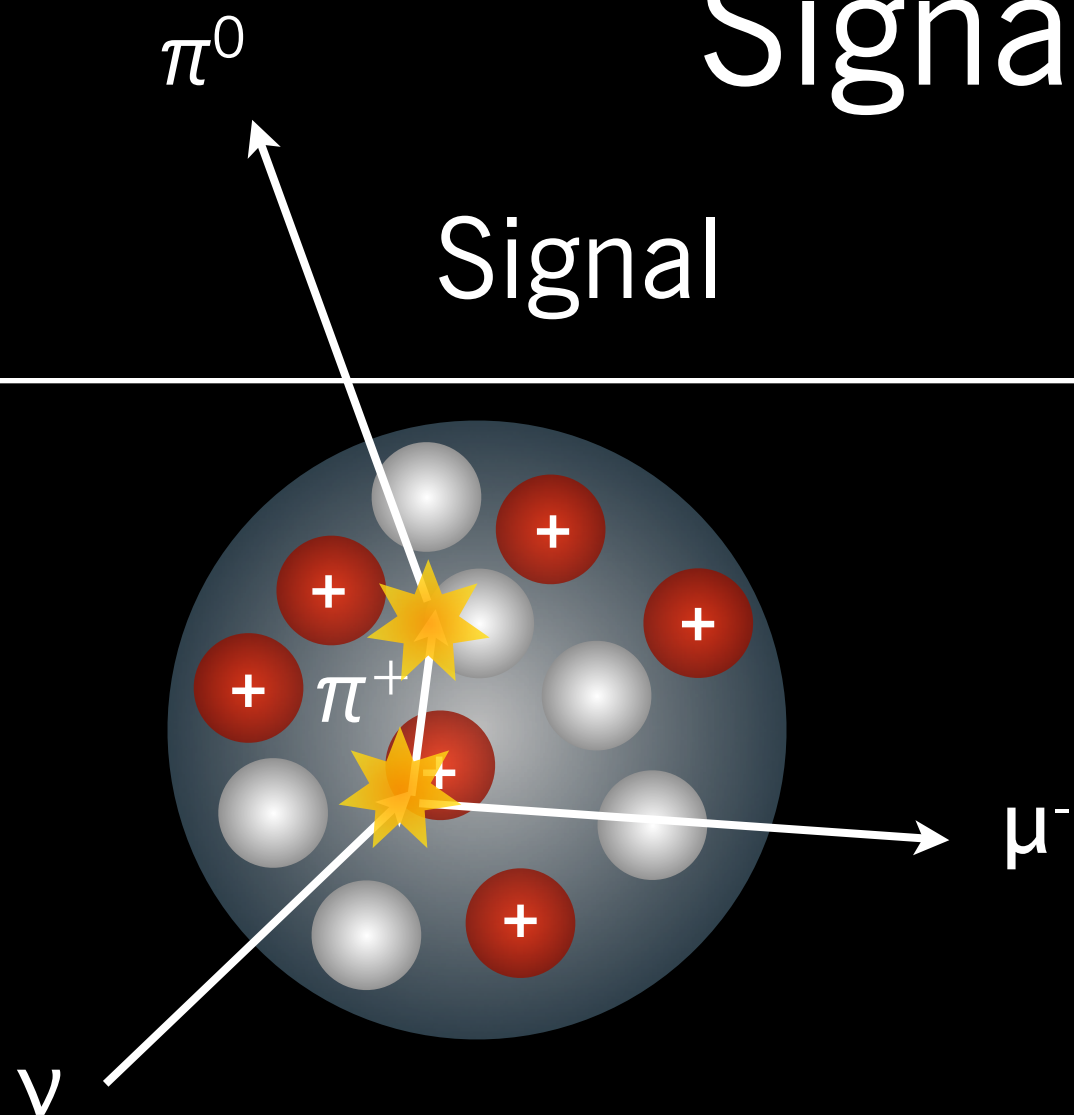
A general concern: final state interaction

- The particles that leave the target nucleus are not necessarily the final state particles from the initial neutrino-nucleon interaction.
- True $CC\pi^+$ can be indistinguishable from CCQE (π^+ absorption) or $CC\pi^0$ (charge exchange).
- Experiments only have access to what came out of the nucleus. These are called **observable events**:
 - An interaction where the target nucleus yields one μ^- , exactly one π^+ , and nuclear debris is *observable* $CC\pi^+$, regardless of the initial nucleon-level interaction
- **Most of our measurements are of observable cross-sections.**



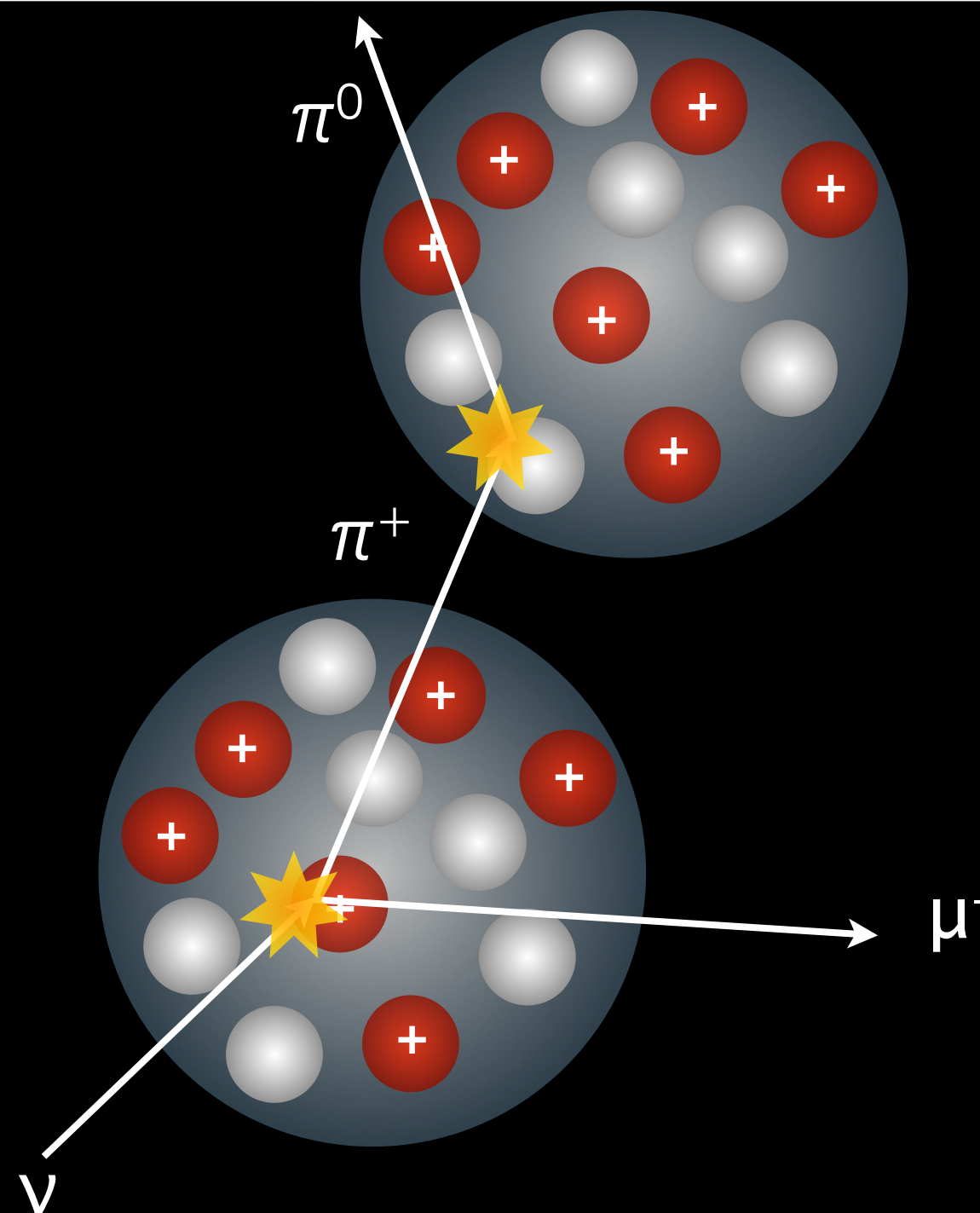
Signal vs tank π^0

Signal



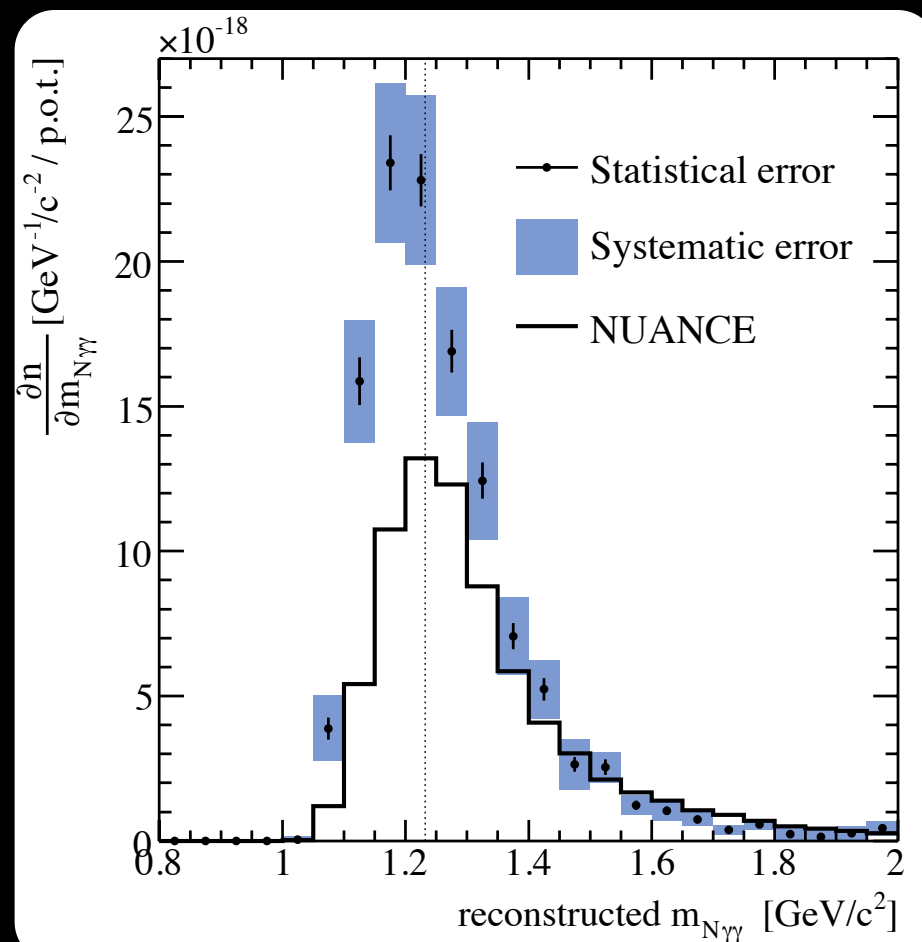
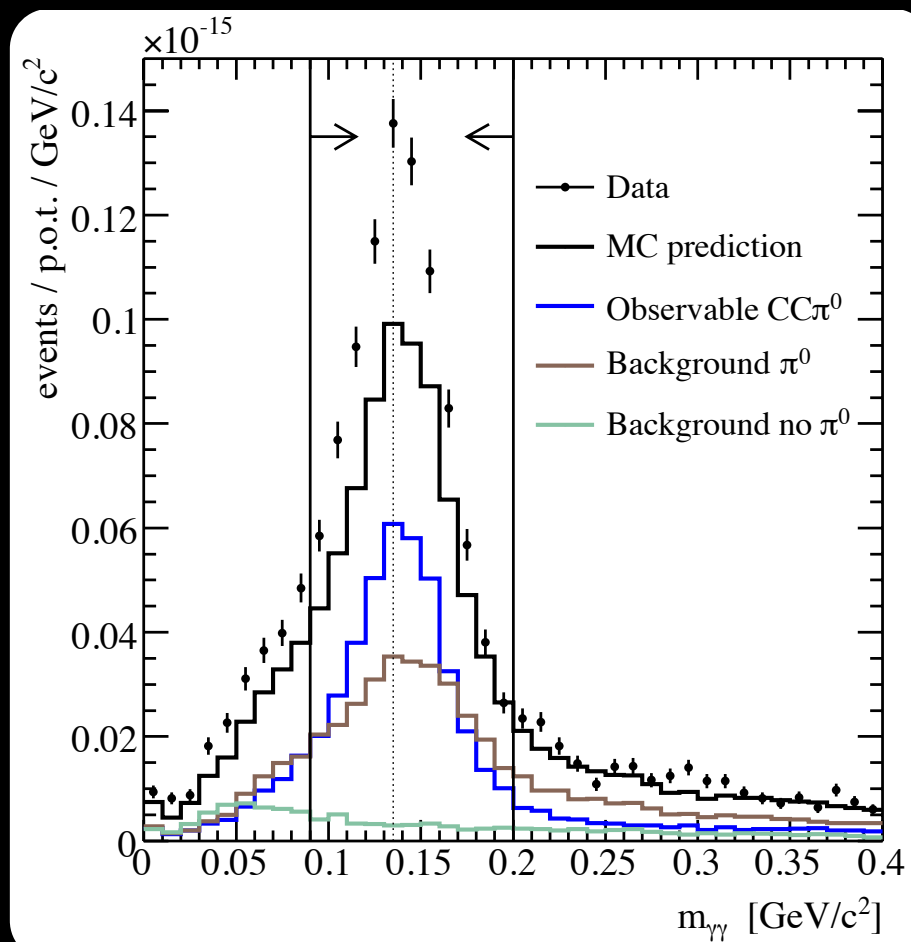
- π^0 from charge exchange within the target nucleus is considered **signal**.
- Charge exchange with *other* nuclei constitutes a **background**.
- We **include** FSI pion production to remove model dependence; **exclude** tank π^0 to remove detector dependence.

Tank π^0



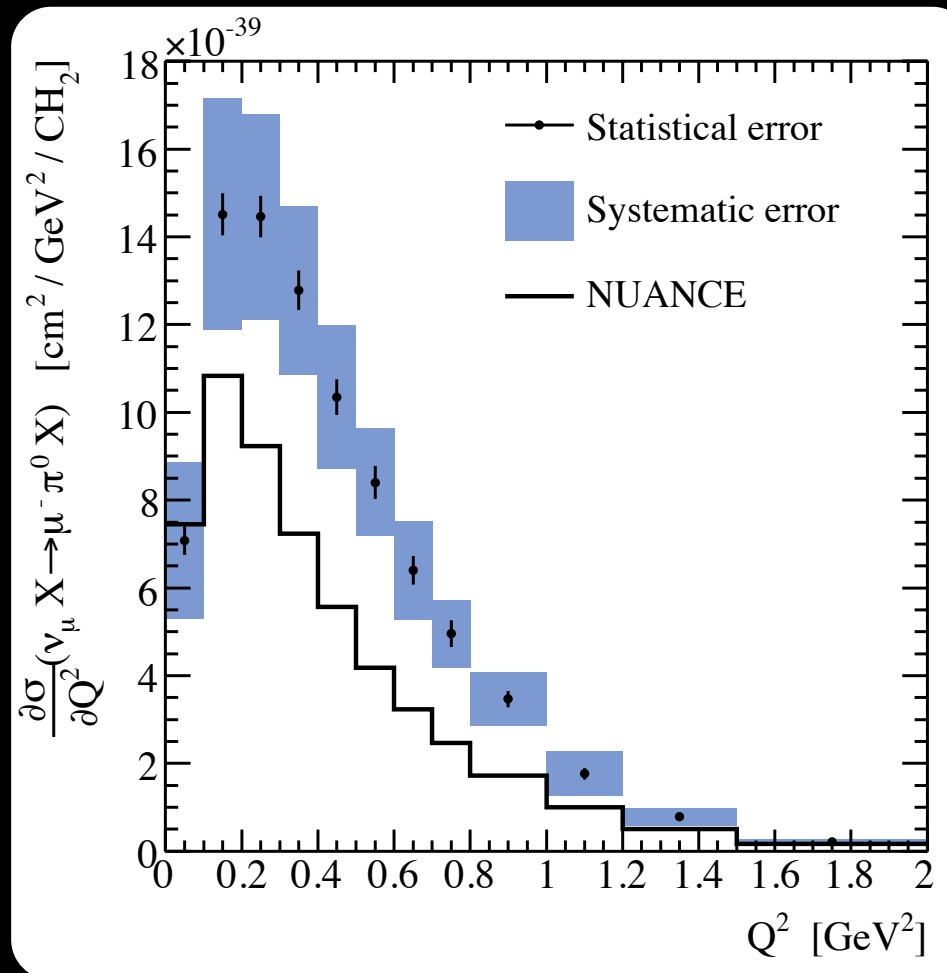
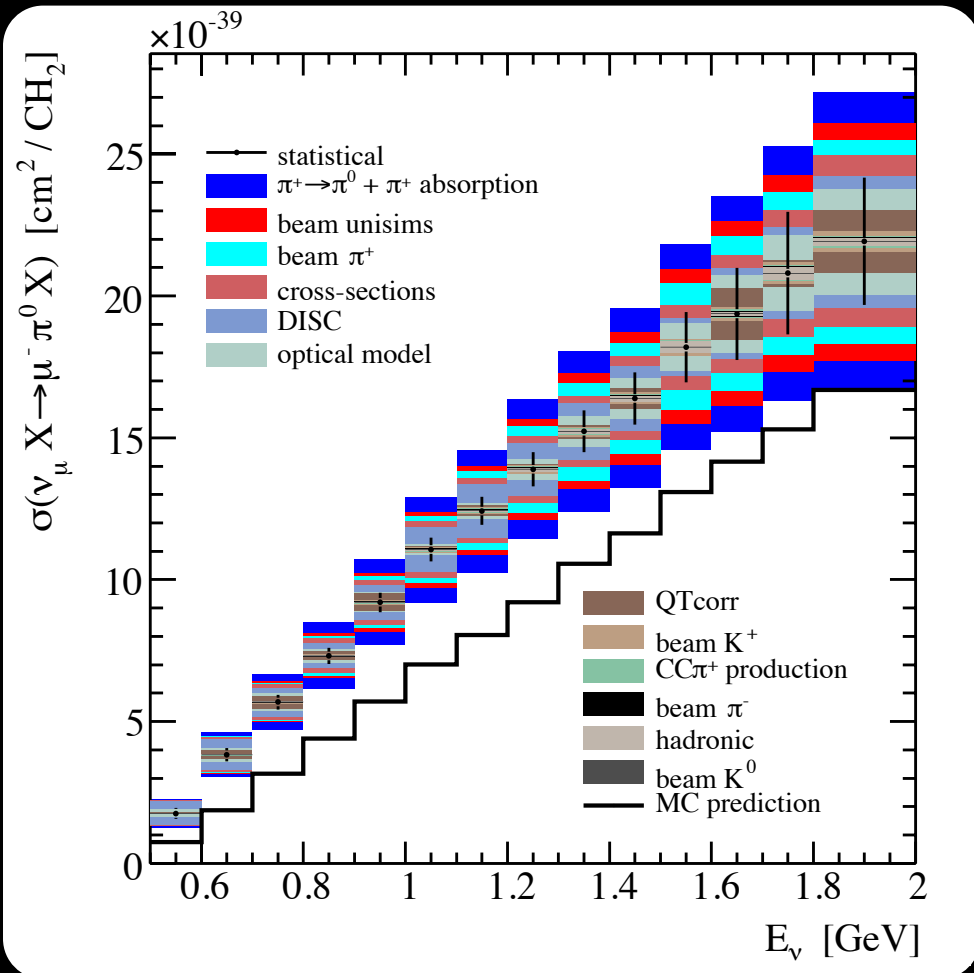
Reconstructed signal candidates

- Two-photon invariant mass $m_{\gamma\gamma}$ allows very effective identification of events with a π^0
- Reconstruction of full event allows observation of Δ resonance



NUANCE is the default MiniBooNE neutrino interaction generator

Measured observable $CC\pi^0$ cross-section



Additionally, we measure differential cross-sections vs:

- θ_μ
- θ_π
- E_μ
- E_π

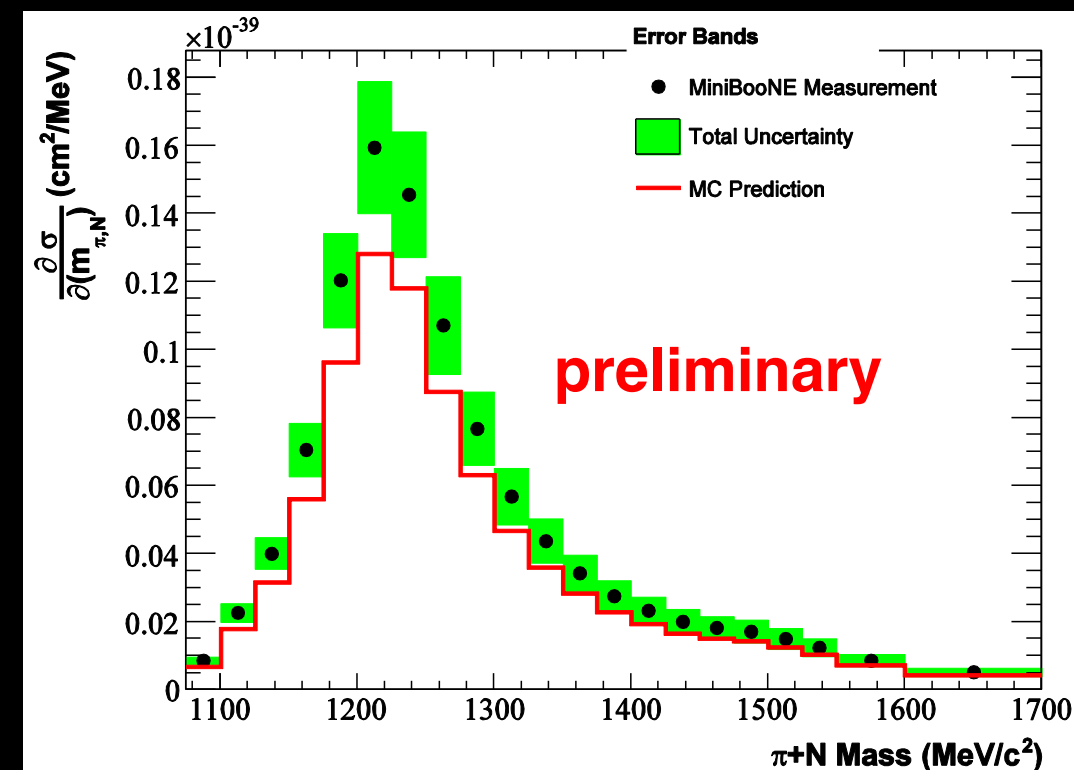
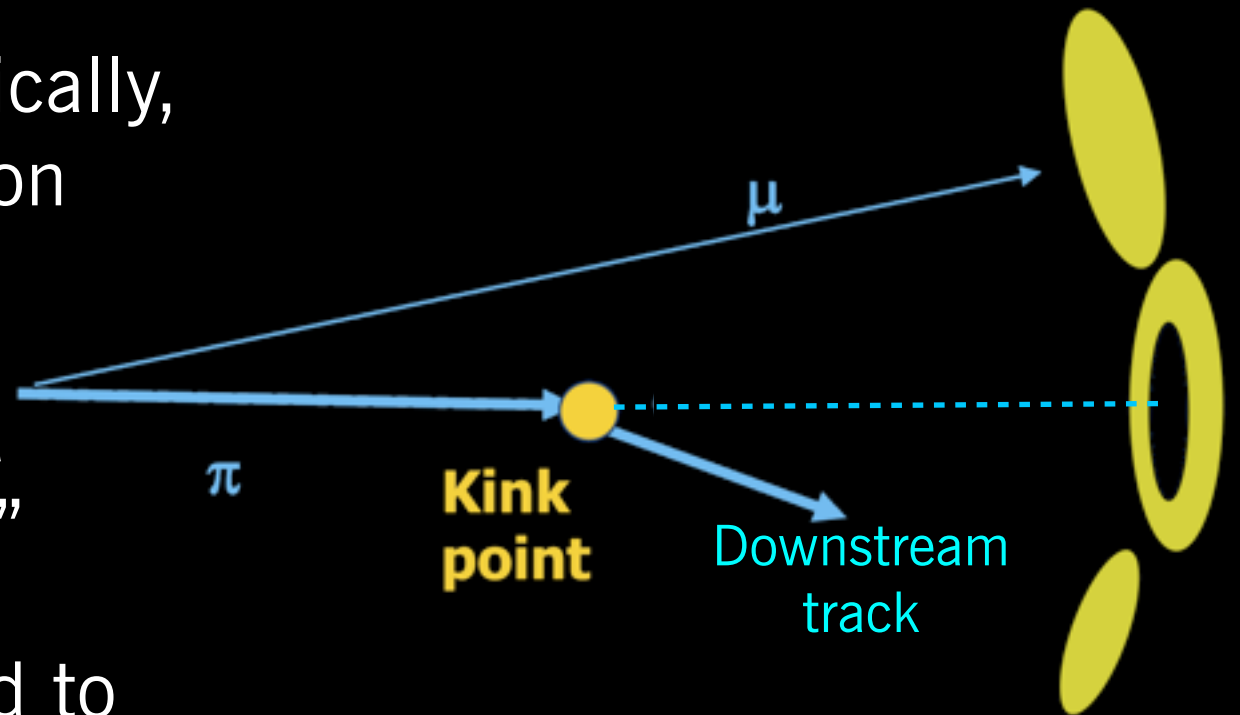
- The dominant error is π^+ charge exchange and absorption in the detector.
- First-ever differential cross-sections on a nuclear target.
- The cross-section is larger than expectation for all energies.
- Publication is imminent.

Charged-current π^+ production

- Second-largest interaction channel at MiniBooNE
- Can proceed via resonance $\nu + N \rightarrow \mu + \Delta \rightarrow \mu + N' + \pi^+$ or by coherent nuclear scatter.
- Identified by observation of *two* stopped muon decays after primary event. Unique signature results in purest exclusive sample in MiniBooNE
- Pion reconstruction and μ/π separation are challenging.

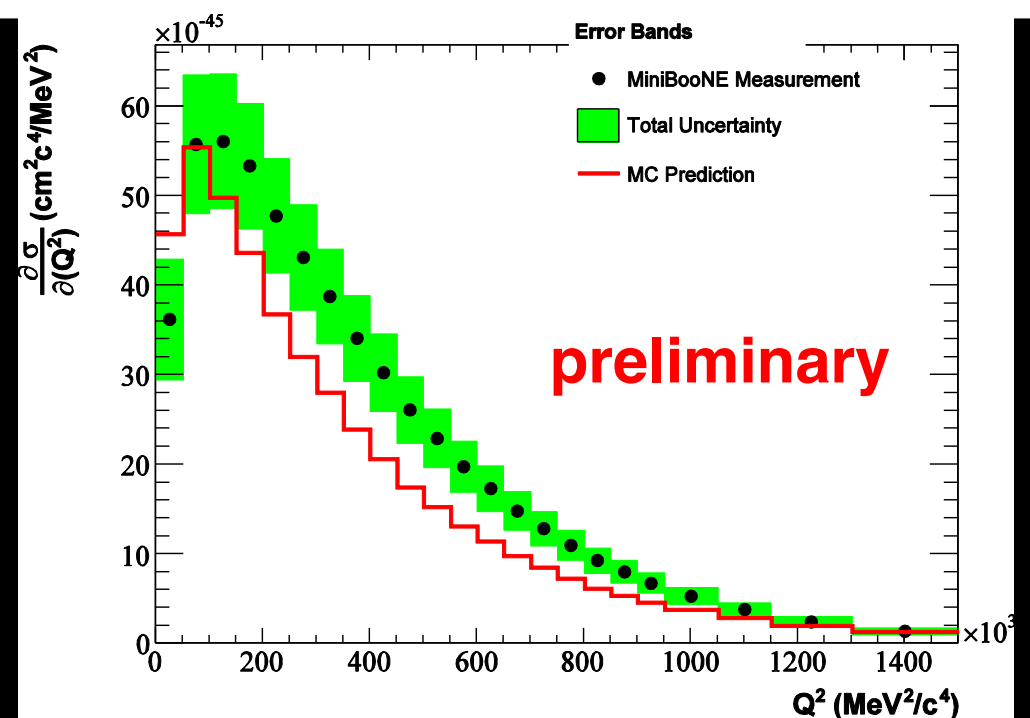
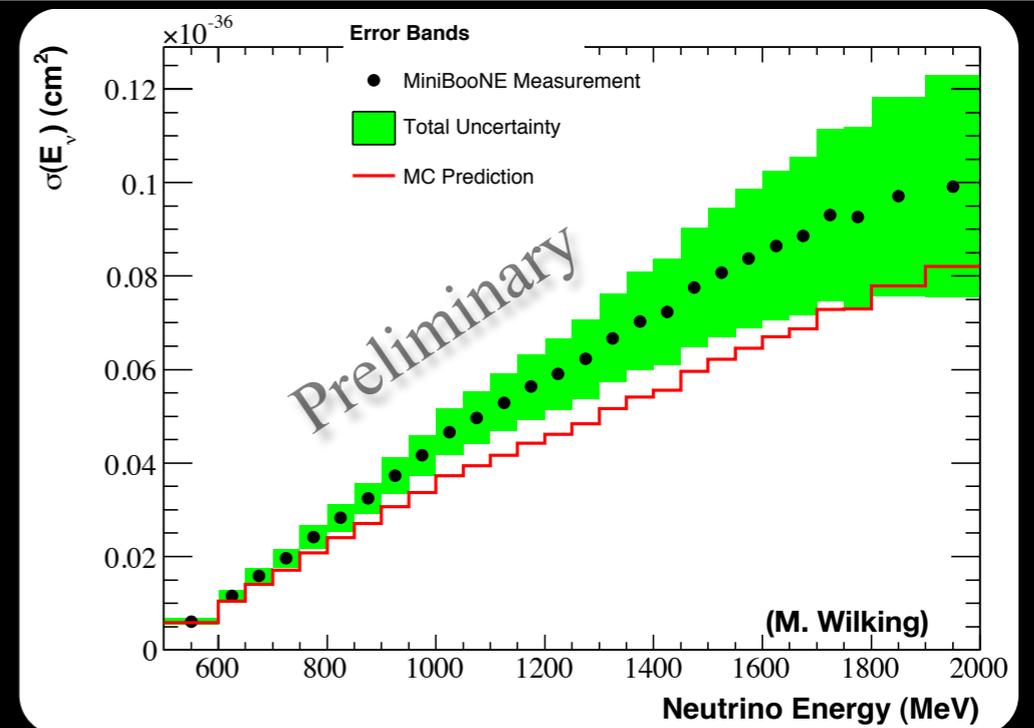
Cherenkov ring shapes: π^+

- Pions occasionally interact hadronically, losing energy and changing direction sharply.
- Kinked track produces two rings: a “doughnut” and a “doughnut hole.”
- Pion reconstruction fitter developed to searched for the kinked track
- Likelihood identifies the pion
- ~90% purity, ~67,000 events.
- Reconstruction of muon and pion allows Δ mass to be calculated



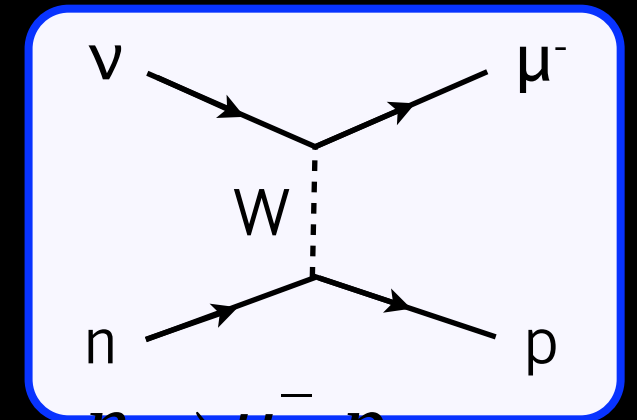
Measured observable charged-current π^+ cross-sections

- Differential cross sections (flux averaged):
 - $d\sigma/dQ^2$, $d\sigma/dE_\mu$, $d\sigma/d\cos\theta_\mu$, $d\sigma/d(E_\pi)$, $d\sigma/d\cos\theta_\pi$:
- Double Differential Cross Sections
 - $d^2\sigma/dE_\mu d\cos\theta_\mu$, $d^2\sigma/dE_\pi d\cos\theta_\pi$
- Data Q^2 shape differs from the model
- Paper submission is imminent



Charged-current quasielastic scattering (CCQE)

- Lepton vertex well understood
- Nucleon vertex parametrized with 2 vector form factors $F_{1,2}$ and one axial vector form factor F_A
- Use relativistic Fermi gas model of nucleus; $F_{1,2}$ come from electron scattering measurements
- Generally assume dipole form of F_A ; only parameter is axial mass m_A extracted from neutrino-deuteron scattering experiments: 2002 average $M_A = 1.026 \pm 0.021$ GeV



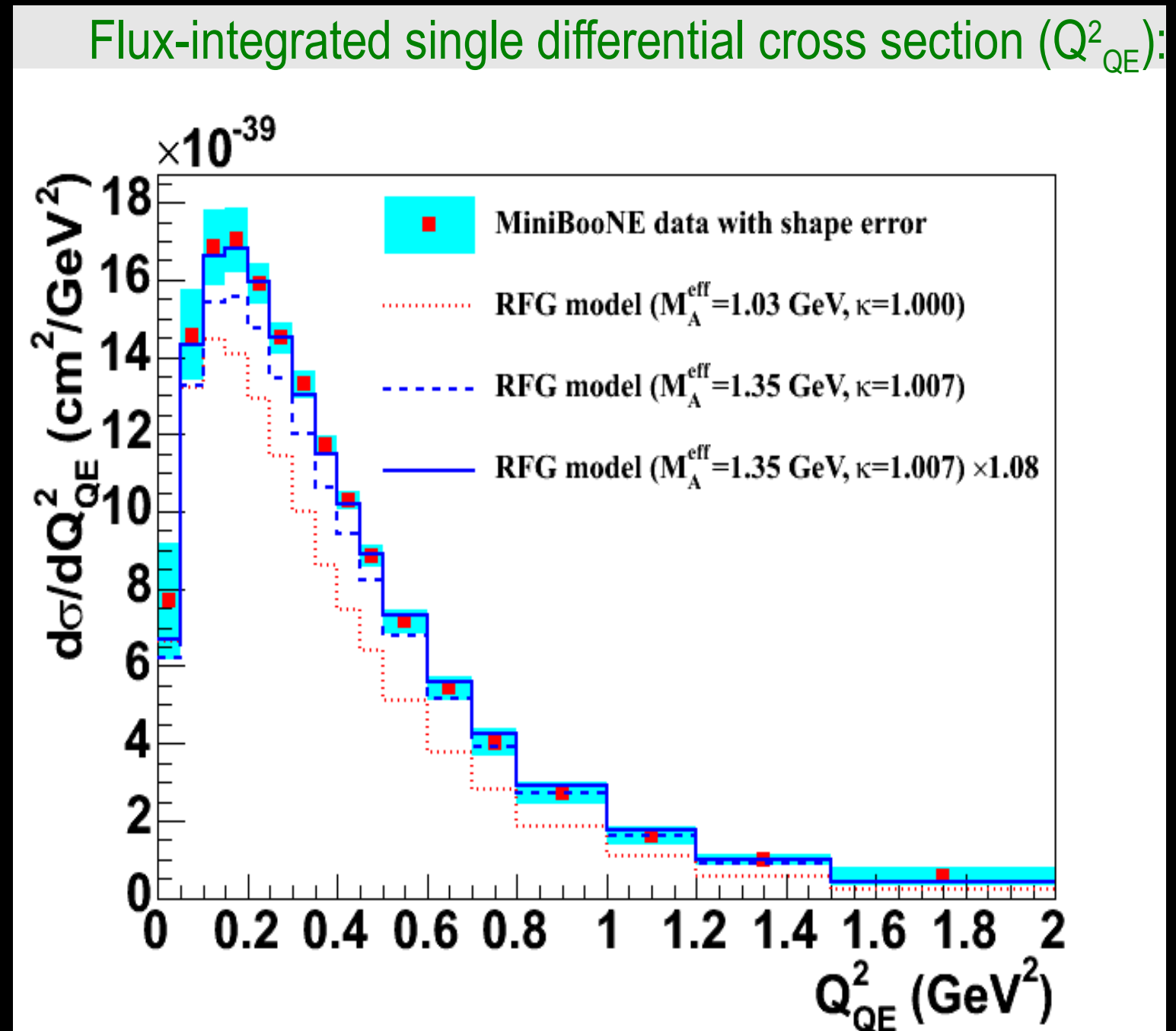
$$F_A(Q^2) = -\frac{g_A}{\left(1 + \frac{Q^2}{M_A^2}\right)^2}$$

CCQE analysis

- We report a nucleon-level cross-section here, not just observable
- $CC\pi^+$ is (largest) background (one μ decay missed because of π absorption, μ -capture, or detector inefficiency)
- Important detail: MiniBooNE data used to measure this background $\sim 1/2$ of $CC\pi^+$ background is irreducible (no π in final state, *i.e.* observable CCQE)
- Final CCQE sample:
 - 146k CCQE candidates
 - 27% efficiency - 77% purity

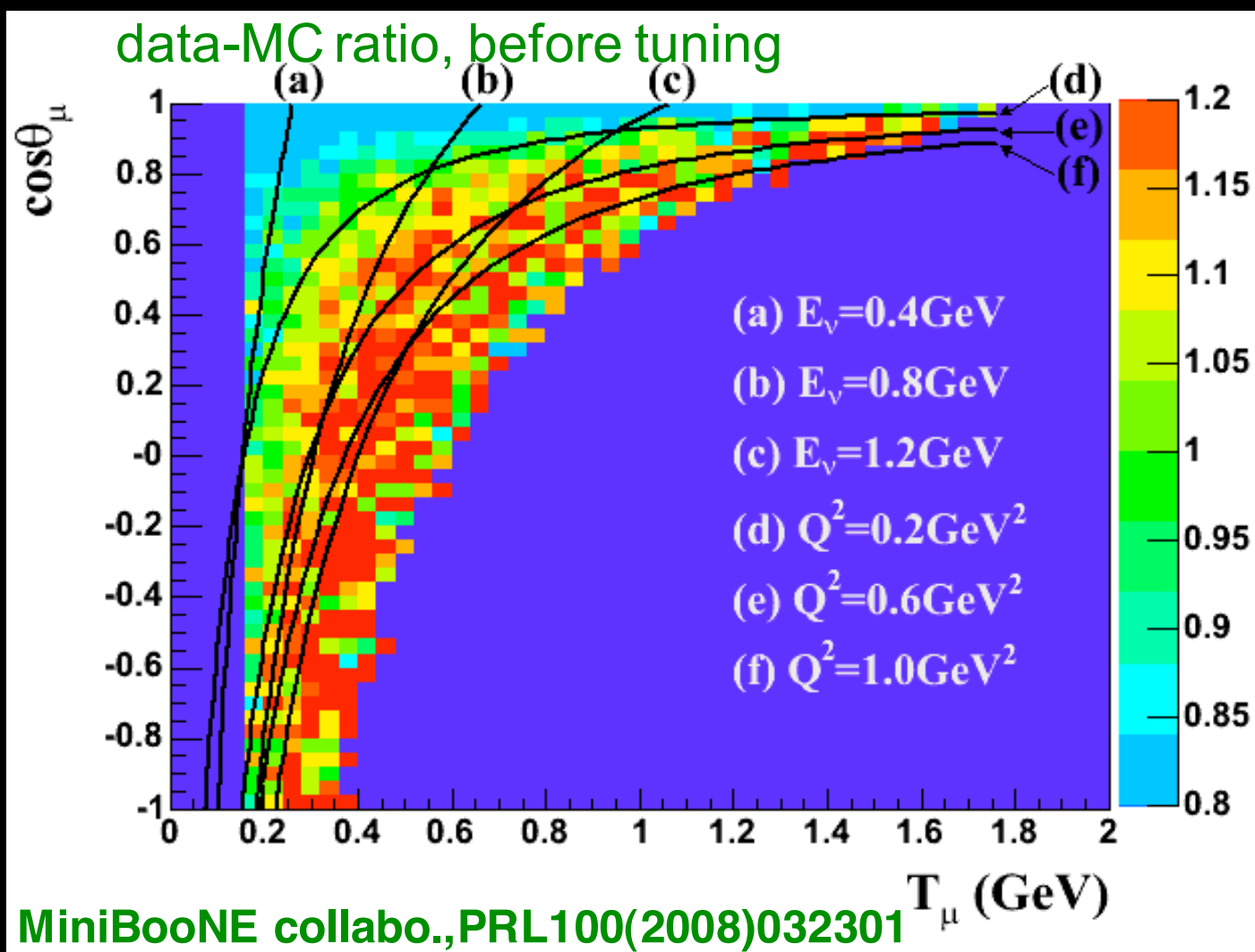
CCQE fit results: Q^2 dependence

- Data are compared (absolutely) with CCQE (RFG) model with various parameter values
- We prefer larger m_A compared to D_2 data
- Our CCQE cross-section is 30% high the world-averaged CCQE model (red).
- Model with CCQE parameters extracted from shape-only fit agrees well with over normalization (to within normalization error).



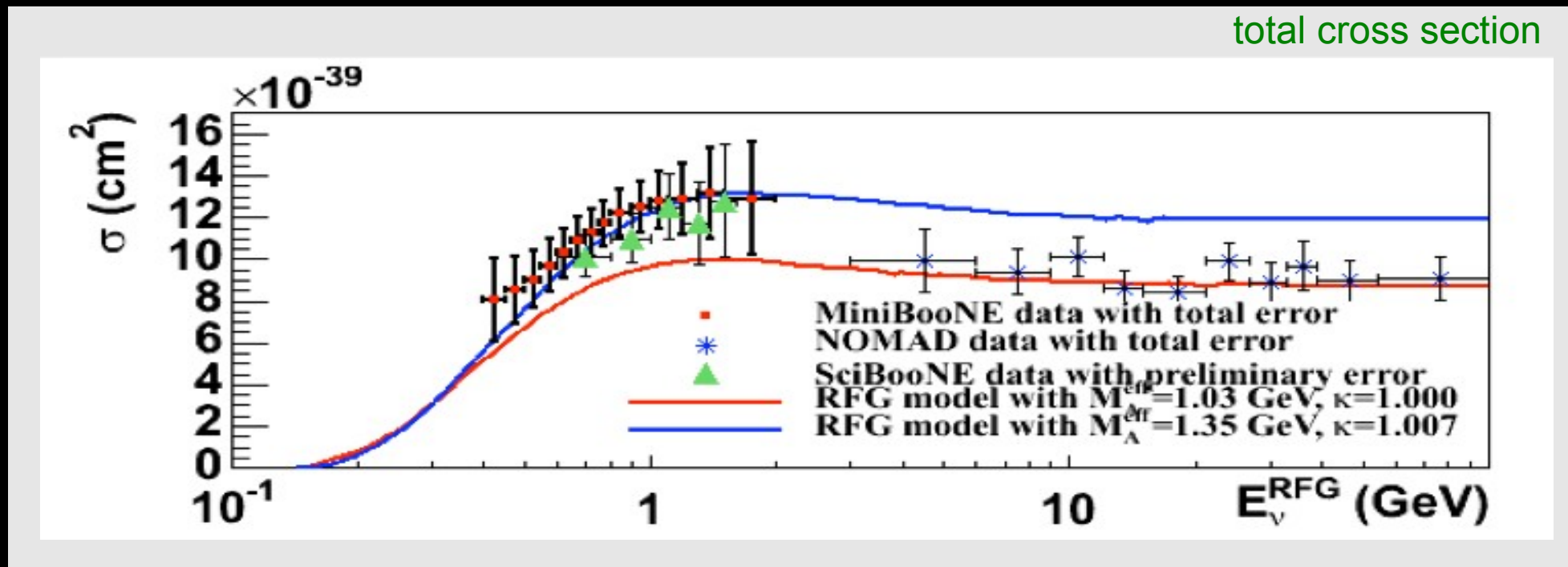
Flux or interaction model?

- Normalization disagrees: check kinematics
- Look at data-MC disagreement before tuning



- Disagreements follow contours of constant Q^2 , not constant E_ν as would be expected if flux wrong.
- Normalization agrees (within errors) with prediction using best fit shape parameters.

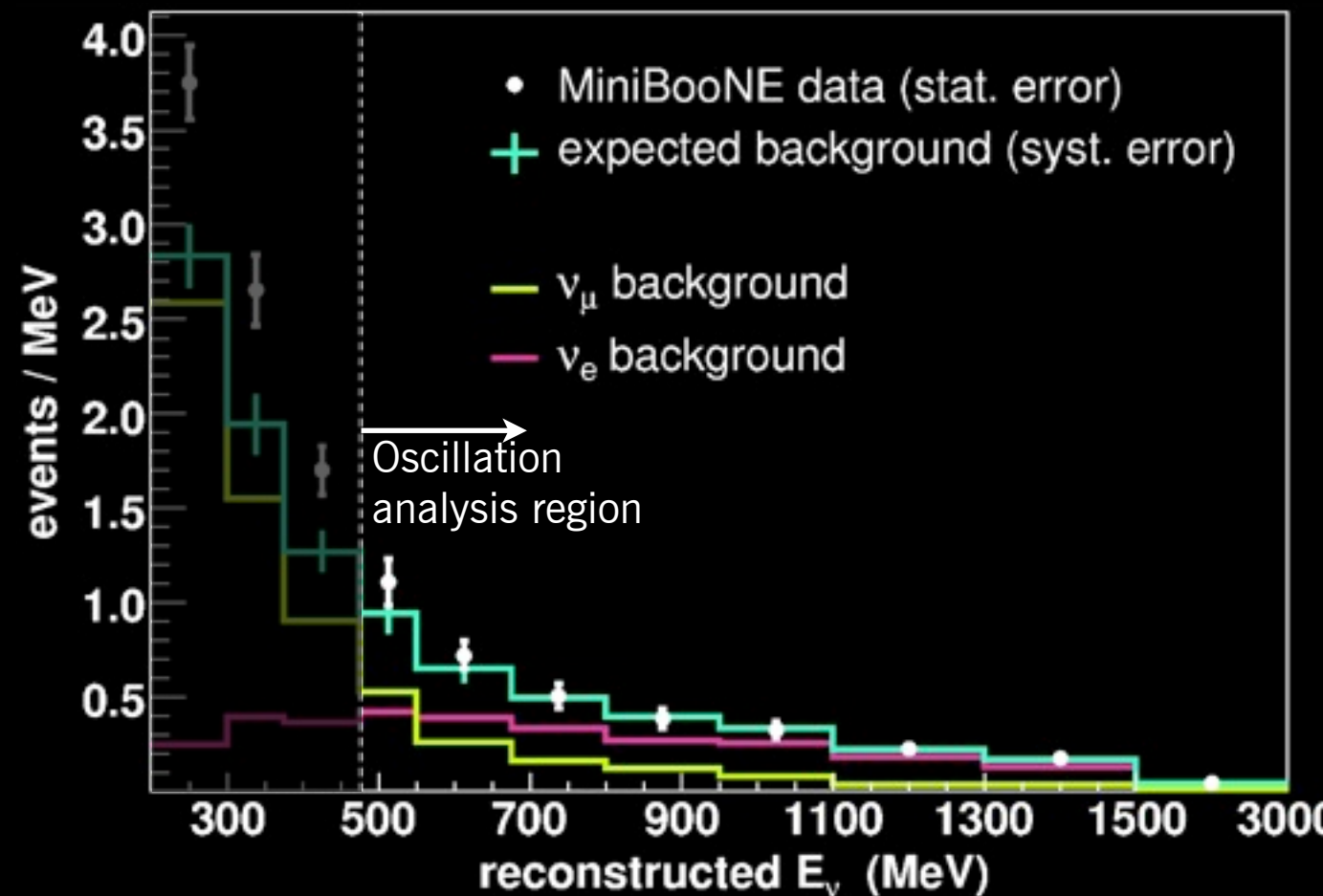
Comparisons to other experiments (carbon targets)



- Our data (and SciBooNE) appear to prefer higher M_A than NOMAD, but the disagreement is not very significant.
- Note that:
 - Our errors are systematic-dominated and grow at highest energies
 - NOMAD required observed muon, proton tracks and no others: in principle, different processes may contribute to the two experiments' samples

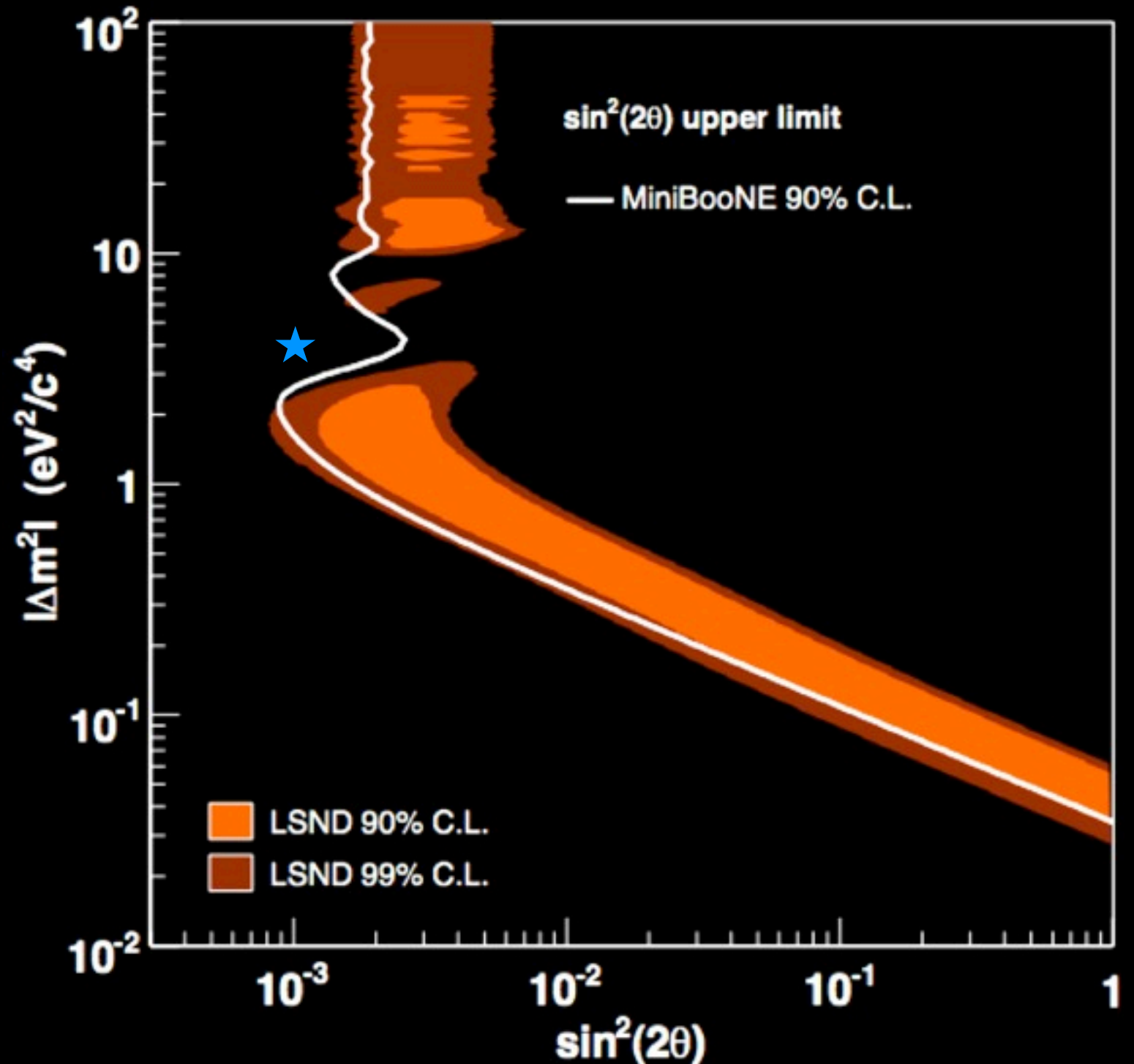
Neutrino Oscillations: 2007 result

- Search for ν_e appearance in the detector using quasielastic scattering candidates
- Sensitivity to LSND-type oscillations is strongest in $475 \text{ MeV} < E < 1250 \text{ MeV}$ range
- Data consistent with background in oscillation fit range
- Significant excess at lower energies: source unknown, consistent with either ν_e or single photon production



Neutrino Oscillation Limit

- Single-sided 90% confidence limit
- Best fit (star):
($\sin^2 2\theta$, Δm^2) =
(0.001, 4 eV²)
- Reported in PRL **98**
231801 (2007)
- Low-energy excess
analysis PRL **102**
101802 (2009)



Antineutrino Oscillations

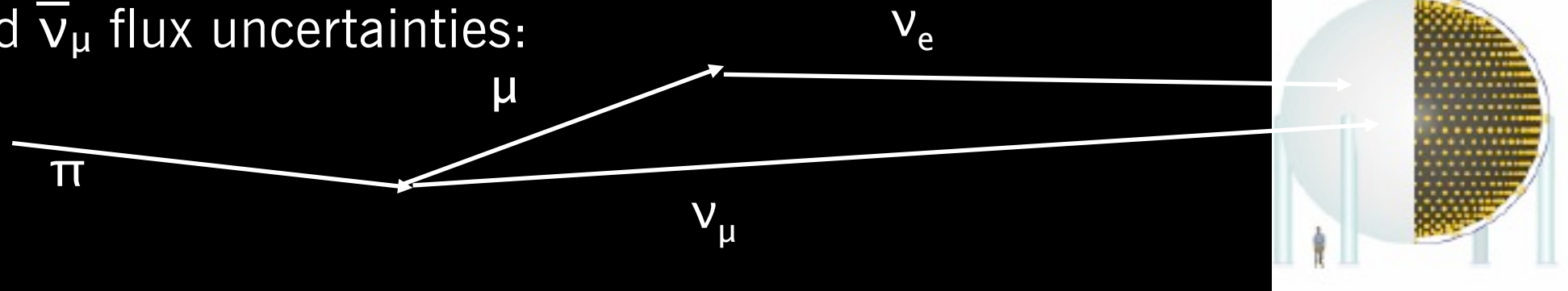
- LSND was primarily an antineutrino oscillation search; need to verify with antineutrinos as well due to potential *CP*-violating explanations
- Now have same number of protons on target in antineutrino vs. neutrino mode, but...
- Antineutrino oscillation search suffers from lower statistics than in neutrino mode due to lower production and interaction cross-sections
- Also, considerable neutrino contamination (20 ± 5)% in antineutrino event sample

Oscillation Fit Method

- Maximum likelihood fit:

$$-2 \ln(L) = (x_1 - \mu_1, \dots, x_n - \mu_n) M^{-1} (x_1 - \mu_1, \dots, x_n - \mu_n)^T + \ln(|M|)$$

- Simultaneously fit
 - $\bar{\nu}_e$ CCQE sample
 - High statistics $\bar{\nu}_\mu$ CCQE sample
- ν_μ CCQE sample constrains many of the uncertainties:
 - $\bar{\nu}_e$ and $\bar{\nu}_\mu$ flux uncertainties:



- Cross section uncertainties (assume lepton universality)

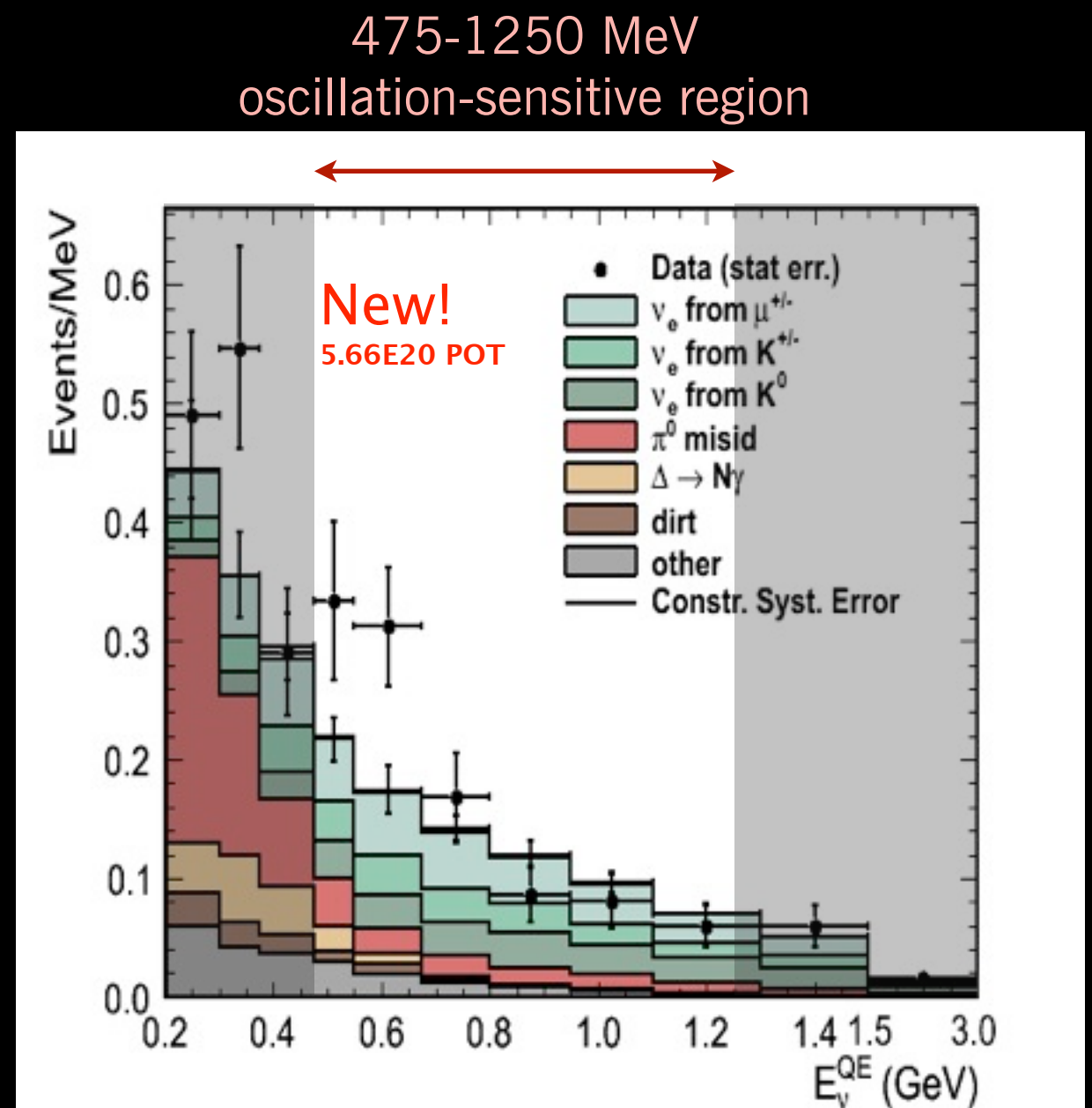
Antineutrino oscillation candidates

- Background modes -- estimate before constraint from $\bar{\nu}_\mu$ data (constraint changes background by about 1%)
- Systematic error on background $\approx 10.5\%$ (energy dependent)

Process	200 – 475 MeV	475 – 1250 MeV
$\bar{\nu}_\mu$ CCQE	4.3	2.0
NC π^0	41.6	12.6
NC $\Delta \rightarrow N\gamma$	12.4	3.4
External Events	6.2	2.6
Other $\bar{\nu}_\mu$	7.1	4.2
$\bar{\nu}_e$ from μ^\pm Decay	13.5	31.4
$\bar{\nu}_e$ from K^\pm Decay	8.2	18.6
$\bar{\nu}_e$ from K_L^0 Decay	5.1	21.2
Other $\bar{\nu}_e$	1.3	2.1
Total Background	99.5	98.1
0.26% $\bar{\nu}_\mu \rightarrow \bar{\nu}_e$	9.1	29.1

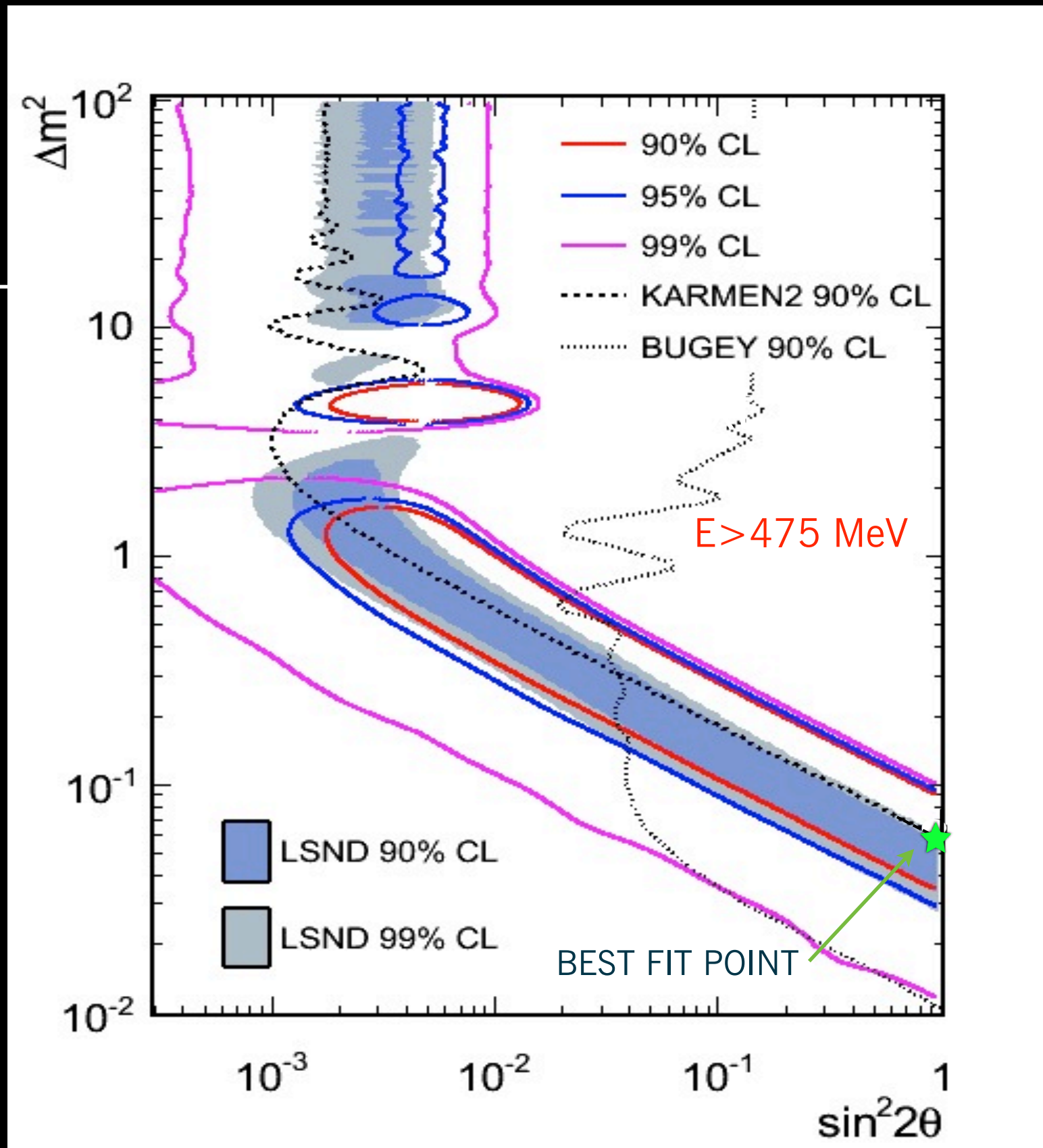
Data in antineutrino oscillation search

- $475 \text{ MeV} < E < 1250 \text{ MeV}$:
 - $99.1 \pm 9.8(\text{syst})$ expected after fit constraints
 - 120 observed
 - Raw counting excess significance is 1.5σ
- Also see small excess at low energy, consistent with neutrino mode excess if attributed to neutrino contamination in $\bar{\nu}$ beam



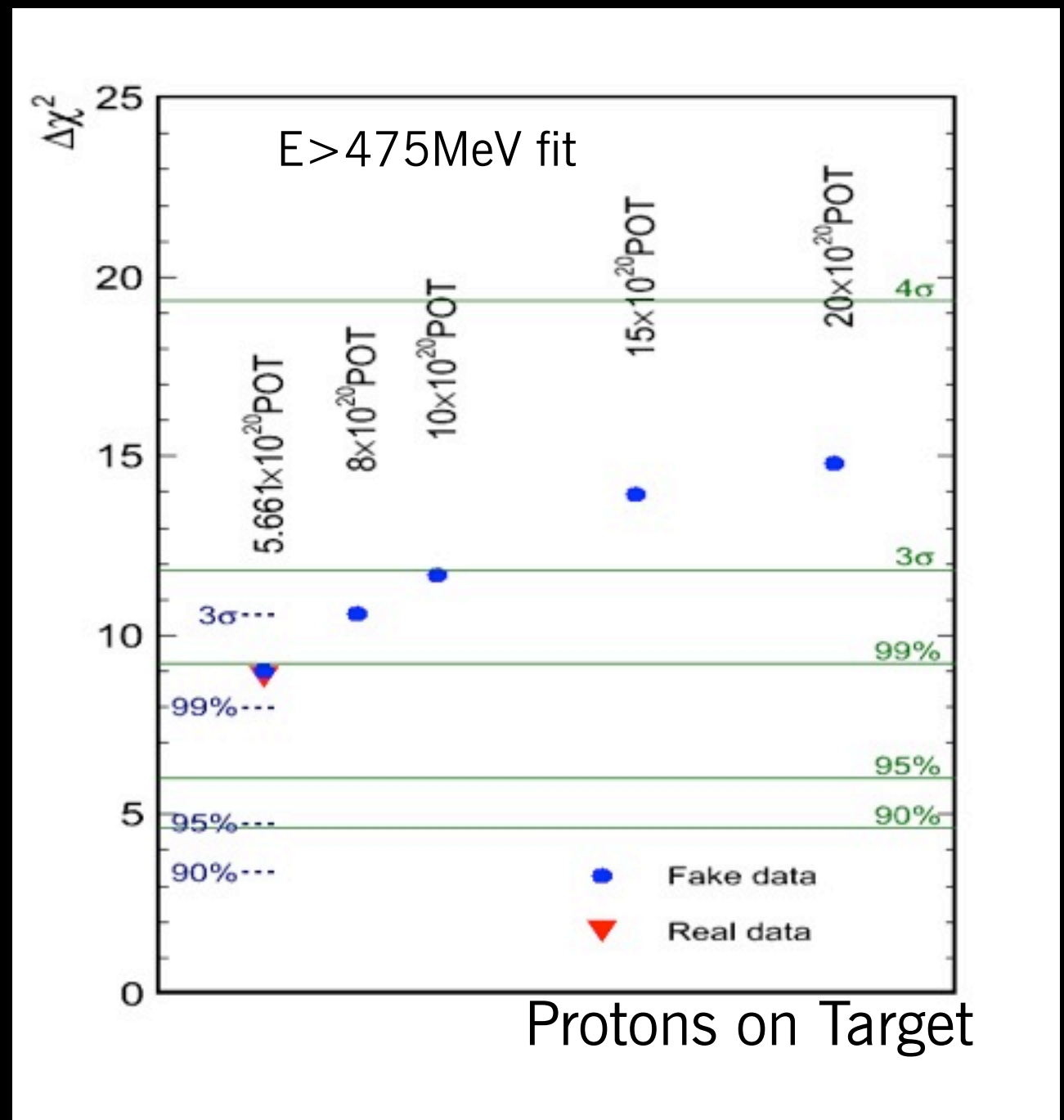
Electron antineutrino appearance oscillation results

- Results for **5.66E20 POT**
- Maximum likelihood fit for *simple two-neutrino model*
- Oscillation hypothesis preferred to background-only at 99.4% confidence level.
- $E > 475$ avoids question of low-energy excess in neutrino mode.
- Signal bins only:
 - $P_{\chi^2}(\text{null}) = 0.5\%$
 - $P_{\chi^2}(\text{best fit}) = \sim 10\%$
- Submitted to PRL
- arXiv: 1007.5510



Future sensitivity in $\bar{\nu}$ data

- MiniBooNE approved for a total of 1×10^{21} POT
- Potential 3σ significance assuming best fit signal
- Systematics limited at about 2×10^{21} POT



Conclusions

- Cross-sections:
 - MiniBooNE has most precise measurements of top five interaction modes on carbon; only differential and double-differential cross-sections in some modes
 - Some disagreements with most common nuclear models?
- Oscillation searches
 - Significant ν_e ($\sim 3 \sigma$) and $\bar{\nu}_e$ ($\sim 2.8 \sigma$) excesses above background are emerging in both neutrino mode and antineutrino mode in MiniBooNE
 - The two modes do not appear to be consistent with a simple two-flavor neutrino model
 - Antineutrino results still heavily statistics-limited; MiniBooNE plans to accumulate more data until the goal of 10^{21} protons on target is reached